

See discussions, stats, and author profiles for this publication at: <https://www.researchgate.net/publication/230827711>

Fe Electron Transfer and Atom Exchange in Goethite: Influence of Al-Substitution and Anion Sorption

ARTICLE in ENVIRONMENTAL SCIENCE & TECHNOLOGY · SEPTEMBER 2012

Impact Factor: 5.33 · DOI: 10.1021/es302094a · Source: PubMed

CITATIONS

23

READS

11

3 AUTHORS, INCLUDING:



Drew Latta

University of Iowa

15 PUBLICATIONS 237 CITATIONS

[SEE PROFILE](#)



Michelle Scherer

University of Iowa

83 PUBLICATIONS 4,120 CITATIONS

[SEE PROFILE](#)

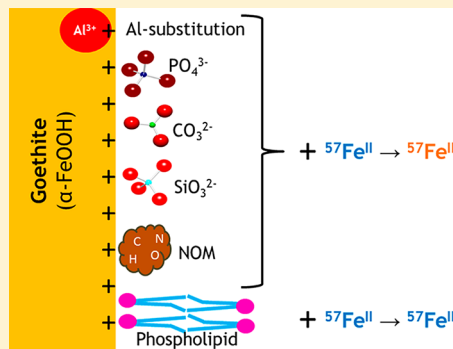
Fe Electron Transfer and Atom Exchange in Goethite: Influence of Al-Substitution and Anion Sorption

Drew E. Latta,^{†,*} Jonathan E. Bachman, and Michelle M. Scherer

Department of Civil and Environmental Engineering, The University of Iowa, Iowa City, Iowa, 52242, United States

Supporting Information

ABSTRACT: The reaction of Fe(II) with Fe(III) oxides and hydroxides is complex and includes sorption of Fe(II) to the oxide, electron transfer between sorbed Fe(II) and structural Fe(III), reductive dissolution coupled to Fe atom exchange, and, in some cases mineral phase transformation. Much of the work investigating electron transfer and atom exchange between aqueous Fe(II) and Fe(III) oxides has been done under relatively simple aqueous conditions in organic buffers to control pH and background electrolytes to control ionic strength. Here, we investigate whether electron transfer is influenced by cation substitution of Al(III) in goethite and the presence of anions such as phosphate, carbonate, silicate, and natural organic matter. Results from ⁵⁷Fe Mössbauer spectroscopy indicate that both Al-substitution (up to 9%) and the presence of common anions (PO₄³⁻, CO₃²⁻, SiO₄⁴⁻, and humic acid) does not inhibit electron transfer between aqueous Fe(II) and Fe(III) in goethite under the conditions we studied. In contrast, sorption of a long-chain phospholipid completely shuts down electron transfer. Using an enriched isotope tracer method, we found that Al-substitution in goethite (10%), does, however, significantly decrease the extent of atom exchange between Fe(II) and goethite (from 43 to 12%) over a month's time. Phosphate, somewhat surprisingly, appears to have little effect on the rate and extent of atom exchange between aqueous Fe(II) and goethite. Our results show that electron transfer between aqueous Fe(II) and solid Fe(III) in goethite can occur under wide range of geochemical conditions, but that the extent of redox-driven Fe atom exchange may be dependent on the presence of substituting cations such as Al.



INTRODUCTION

Iron (Fe) is the fourth most abundant element in the Earth's crust, and the single most abundant redox active metal in the terrestrial environment. Cycling of Fe oxidation states is linked to the modern cycling of globally important elements, such as carbon¹—including xenobiotic compounds²—nitrogen,³ phosphorus,⁴ and the ancient cycling of oxygen.⁵ Fe(II) is produced in the subsurface under anoxic conditions by the action of dissimilatory Fe reducing bacteria (DIRB) coupled to oxidation of organic carbon,² and during coupled biotic/abiotic weathering of minerals.⁶ Fe(II) is significantly more soluble and mobile than Fe(III) and has been shown to sorb to mineral surfaces (e.g., ref 7), catalyze reduction of environmental contaminants in the sorbed state,^{7,8} and lead to recrystallization or secondary mineralization of Fe oxides such as ferrihydrite, schwertmannite, jarosite, and lepidocrocite to goethite, magnetite, and green rust.^{9–13}

A growing body of research points to complex redox-driven dynamics when Fe(II) reacts with Fe(III) oxides, which includes sorption of Fe(II) to the oxide (e.g., refs 8 and 14), electron transfer between sorbed Fe(II) and structural Fe(III) (e.g., refs 15–17), reductive dissolution coupled to oxidative growth and atom exchange (e.g., refs 11,18–20), and in some cases, mineral phase transformation (e.g., ref 10 (for a recent review see Gorski and Scherer (2011)²¹). For oxides where there is no indication of secondary mineralization after reaction

with aqueous Fe(II) (e.g., goethite¹⁸ and magnetite²²), but extensive atom exchange and recrystallization still occurs, we have proposed a redox-driven conveyor belt concept to explain how such extensive Fe atom exchange occurs in the absence of any phase transformation or change in the size or shape.¹⁸ The redox-driven conveyor belt model involves spatially separated oxidative sorption and reductive dissolution linked by bulk conduction¹⁹ (or in the case of magnetite possibly by Fe(II) diffusion²²) through the mineral.

Evidence of such extensive recrystallization during reaction with Fe(II) compels us to acknowledge that the oxide is not merely a static surface in the sorption reaction, but that reaction with Fe(II) causes time dependent changes to the Fe(III) oxide. Studies showing the release and incorporation of metals to and from solution in the presence of aqueous Fe(II) and Fe oxides (Ni, Co, Zn, As, and U), as well as oxidation of As(III) to As(V), indicate the complexity of reactions that electron transfer and atom exchange induce.^{13,22–27} Efforts are being made to incorporate Fe(II)–Fe(III) electron transfer reactions into surface complexation models,²⁸ and represent a step

Received: May 25, 2012

Revised: August 1, 2012

Accepted: August 27, 2012

Published: September 10, 2012



forward in prediction of Fe redox dynamics in reducing environments.

While a significant body of work has emerged demonstrating electron transfer and atom exchange between aqueous Fe(II) and Fe(III) oxides,²¹ much of the work to date has been done with pure oxides in simple solutions containing only a buffer and background electrolyte so that the interaction between Fe(II) and Fe(III) can be isolated, with fewer studies investigating more complex systems.^{12,29–32} Here, we investigate whether electron transfer and Fe atom exchange can occur under more complex conditions found in the natural environment. It is well-known that Fe oxides in the environment can incorporate various cations into their structure, particularly the highly abundant Al(III) cation.^{33,34} Research on both natural and synthetic aluminum substituted goethites (Al-goethites) suggest that approximately 33% of the Fe(III) in goethite can be replaced by Al (i.e., Al/(Al+Fe) up to 33%).³⁴ Al-substitution in goethite has been shown to inhibit reductive dissolution of goethites by dithionite (e.g., ref 35). The influence of Al-substitution on rates of biological reduction of goethite by DIRB is less clear, with some observing decreased rates of reduction as Al substitution increases,³⁶ to others observing no effect of Al-substitution.³⁷

Anions present in the environment, such as carbonate, phosphate, silicate, and natural organic matter, can also sorb to goethite and influence its reactivity.^{38–42} Phosphate (PO_4^{3-}) has been the subject of a large number of studies due to its importance in determining soil fertility, for example, refs 41 and 42. The inner-sphere sorption of the phosphate anion changes the surface charging characteristics of goethite suspensions, and makes the goethite surface have a higher affinity for cations.^{42–45} Sorbed phosphate has also been shown to inhibit reductive dissolution of goethite by DIRB,⁴⁶ and has a pronounced effect on Fe oxide secondary mineralization pathways (e.g., refs 47 and 48).

In this study, we use ^{57}Fe Mössbauer spectroscopy to investigate whether electron transfer between Fe(II) and structural Fe(III) in goethite is influenced by cation substitution of Al(III) in goethite and the presence of anions such as phosphate, carbonate, silicate, and natural organic matter, as well as a long-chain phospholipid. We also use an ^{57}Fe enriched isotope tracer approach to investigate whether Fe atom exchange is influenced by both Al-substitution in goethite and sorbed phosphate. We demonstrate that both Al-substitution (up to 10%) and the presence of common anions (PO_4^{3-} , CO_3^{2-} , SiO_4^{4-} , and humic acid) does not inhibit electron transfer between aqueous Fe(II) and Fe(III) in goethite, whereas the long-chain phospholipid shuts down electron transfer. Al-substitution in goethite (~10%), does, however, significantly decrease the extent of atom exchange between Fe(II) and goethite (from 43 to 12%). Phosphate, somewhat surprisingly, appears to have little effect on the rate and extent of atom exchange between aqueous Fe(II) and goethite.

MATERIALS AND METHODS

Goethite Synthesis and Characterization. Goethite was synthesized from naturally abundant iron with and without aluminum substitution by modifying previously described methods.^{49,50} Synthesis parameters are summarized in Table S1 in the Supporting Information (SI). Nanometer-sized goethite (nanogoethite) synthesis is described in our previous work, and is a modification of procedures described by Burleson and Penn.^{51,52} Al-free goethite and Al-substituted

goethite were prepared from $^{56}\text{Fe}(0)$ in a similar manner, with modifications based on the source of Fe. Further details are provided in the SI.

Goethite was the only phase detected using Mössbauer spectroscopy (SI Figure S1) and powder X-ray diffraction (pXRD) (SI Figure S2). Goethites synthesized with ^{56}Fe had negligible Mössbauer signal. Scanning electron microscopy (SEM) provided morphology and particle size information (SI Figure S3). Additional details on characterization are given in the SI and summarized in Table S1. In summary, Al-contents measured by dissolution were 9.9% (10% Al-Goethite) for naturally abundant Fe Al-goethite, and 5.4% and 9.4% for the ^{56}Fe Al-goethites used (referred to as “ ^{56}Fe Al-goethite (5%)” and “ ^{56}Fe Al-goethite (9%)”). When the amount of material synthesized permitted, dissolution experiments were done to check for congruent dissolution (SI Figure S4). Dissolution of Fe and Al from the goethite was congruent.

Electron Transfer Experiments. Mössbauer experiments tracking electron transfer between Fe(II) and goethite and Al-goethite were done in an anoxic glovebox (93% N₂/7% H₂) with a Pd catalyst to remove trace oxygen. A stock of 0.1 M $^{57}\text{Fe}(\text{II})$ was made by dissolving $^{57}\text{Fe}(0)$ (Chemgas, Inc., 97.82% ^{57}Fe purity) in HCl in a sealed serum bottle at 70 °C for 2 weeks. Experiments were done in reactors containing 12.5 mL of 25 mM HEPES buffer (4-(2-hydroxyethyl)piperazine-1-ethanesulfonic acid, *N*-(2-hydroxyethyl)piperazine-*N'*-(2-ethanesulfonic acid) with 25 mM KBr as a background electrolyte. The pH was set to a value of 7.5 using 0.1 M KOH. Aliquots of $^{57}\text{Fe}(\text{II})$ stock were added to make nominal Fe(II) concentrations of 1 and 3 mM. The initial concentration of Fe(II) was measured and 25 mg ^{56}Fe goethite and ^{56}Fe Al-substituted goethite was added for a solids loading of 2 g L⁻¹. Reactors were placed on an end-over-end rotator and sampled after 20 h of reaction. Samples for Mössbauer analysis were collected on a 0.45 μm cellulose acetate filter and sealed between two pieces of Kapton tape and quickly transferred to the spectrometer for analysis. Details on Mössbauer analysis are provided in the SI.

To investigate the effect of sorbed anions on electron transfer between Fe(II) and Fe(III) in goethite, experiments were done using 12.5 mL of 10 mM KCl solution at pH 7.5 and 25 mg ^{56}Fe goethite for a solids loading of 2 g L⁻¹. Anions were added from stocks of KH₂PO₄ (100 mM), sodium bicarbonate (1 M), freshly prepared sodium orthosilicate (100 mM Na₄SiO₄), and Aldrich humic acid (200 mg/L). In all cases the anion was presorbed to the goethite, and Fe(II) was added subsequently to the goethite and anion suspension. For experiments with the phospholipid (1,2-dioleoyl-sn-glycerol-3-phosphate or DOPA, Avanti Polar Lipids) a ~1 mM DOPA and goethite suspension was preprocessed by sonication in a bath sonicator at room temperature for 2 h. The phospholipid experiment was done in 25 mM HEPES buffer containing 25 mM KBr adjusted to pH 7.5. The initial concentration of Fe(II) was determined in parallel in reactors without goethite.

After 4–8 h of reaction the samples were filtered for Mössbauer analysis and the final aqueous Fe(II) and PO₄³⁻ (where present) was measured. Experimental conditions, including anion concentrations and Fe(II) concentrations are summarized in SI Table S2. Phosphate was measured using a reduced volume modification of the Standard Methods procedure “4500-P.E. Ascorbic Acid Method” such that 1 mL of sample and 0.16 mL of the combined reagent solution were used.⁵³ Fe(II) was measured using 1,10-phenanthroline with

masking of Fe(III) by fluoride, when required.⁵⁴ Total Fe was measured by reduction of Fe(III) by hydroxylamine hydrochloride to Fe(II).

Isotope Exchange Experiments. Isotope exchange experiments between ⁵⁷Fe(II) spikes and goethite with a natural isotope composition were conducted under similar conditions as the Mössbauer spectroscopy experiments. For the goethite and Al-goethite isotope exchange experiments, an aliquot of the ⁵⁷Fe(II)Cl₂ solution was added to give an approximate concentration of 1 mM Fe(II) in 15 mL of 25 mM HEPES buffer containing 25 mM KBr as a supporting electrolyte, and the pH was adjusted back to a value of 7.5 with 0.1 M KOH. A sample was withdrawn at this point for the initial isotope composition and aqueous Fe(II) concentration. Then, 30 mg (± 0.3 mg) of goethite (Batch 2, SI Table S1) or 10% Al-goethite was added to initiate the reaction. Triplicate 20 mL serum vial reactors were allowed to react for 10 min to 32 days in the anoxic chamber. After the reaction, the contents of the serum vials were transferred to Oak Ridge style centrifuge tubes and sealed with an O-ring and Teflon tape. The reactors were centrifuged outside the glovebox at 12 000 \times g for 5 min and immediately returned to the glovebox. The supernatant was decanted off the pelleted goethite, filtered past a 0.22 μ m filter, and acidified with 50 μ L concentrated HCl. The pellet was dissolved in 4 mL concentrated HCl and diluted with DI water to a final volume of 20 mL.

Isotope exchange experiments were also done in the presence of phosphate and Fe(II). Experiments were conducted with 1 g L⁻¹ suspensions of nanogoethite in 10 mM KCl adjusted to pH 7.5 and pre-equilibrated with 0.35 mM phosphate overnight. After equilibration with phosphate, a nominal concentration of 0.1 mM ⁵⁷Fe(II) was added to the suspensions. Initial Fe(II) concentrations and isotope compositions were measured on triplicate control reactors without goethite and phosphate. Final Fe(II) and phosphate concentrations were measured as described above. In addition, we measured a phosphate sorption isotherm in the absence of Fe(II) at pH 7.5 in 10 mM KCl by varying the initial concentration of PO₄³⁻.

Isotope analysis was performed with a Thermo Fisher Scientific X Series 2 Quadrupole ICP-Mass Spectrometer operating in collision cell mode with a glass concentric nebulizer and a HEPA filtered autosampler. Collision cell gas was 7% H₂, 93% He (>99.996% pure) with a flow rate of 1 mL min⁻¹ to remove the isobaric interference of ¹⁶O/⁴⁰Ar with ⁵⁶Fe. Aqueous and solid phase Fe isotope measurements were done by diluting to a total Fe concentration of approximately 30 ppm in 0.1 M HCl. Dilution kept the signal on all Fe isotopes in the pulse-counting mode on the mass detector and avoided linearity issues in converting the signal response between pulse-counting and analog voltage detection modes. Changes in instrumental detection efficiency were monitored using an internal spike of 10 ppb ⁵⁹Co. Typical changes in ⁵⁹Co detection over a run were less than 2%, with no discernible trend, therefore no correction to measured Fe counts was made. Fe isotope fractions were calculated by dividing the counts in each isotope channel by the sum of the total counts over all four channels (masses of 54, 56, 57, and 58). The fraction of isotope *i* is given by:

$$f^i \text{Fe} = \frac{i \text{counts}}{\text{54 counts} + \text{56 Counts} + \text{57 counts} + \text{58 counts}} \quad (1)$$

RESULTS AND DISCUSSION

Influence of Al-Substitution on Fe(II)-Goethite Electron Transfer. We have used the isotope specificity of ⁵⁷Fe Mössbauer spectroscopy to investigate whether electron transfer occurred between aqueous Fe(II) and Fe(III) in Al-substituted goethite. Specifically, we reacted 1 mM and 3 mM aqueous ⁵⁷Fe(II) with 2 g L⁻¹ suspensions of Mössbauer invisible ⁵⁶Fe goethite and ⁵⁶Fe Al-goethite (5 and 9 mol % Al) in pH 7.5, 25 mM HEPES, and 25 mM KBr buffer. By exploiting the isotope specificity of the Mössbauer technique, we are able to track the change in speciation of the added ⁵⁷Fe(II) after sorption to the Mössbauer-invisible ⁵⁶Fe (Al-substituted) goethite (ref 21 and references therein). Average sorption of Fe(II) from solution by the goethite and Al-goethite observed for 1 mM Fe(II) and 3 mM Fe(II), respectively, was on the order of 0.13 ± 0.014 and 0.18 ± 0.05 mmol/g (1σ) with no clear trend that increasing amounts of Al-substitution influenced Fe(II) sorption.

After reaction with ⁵⁷Fe(II), the Mössbauer spectra of the Al-goethites are predominantly Fe(III) in nature, based on center shift values between 0.43 and 0.50 mm s⁻¹, and are similar to a goethite standard (Figure 1A–C).⁵⁵ The primarily Fe(III) character of the spectral features indicates that most of the

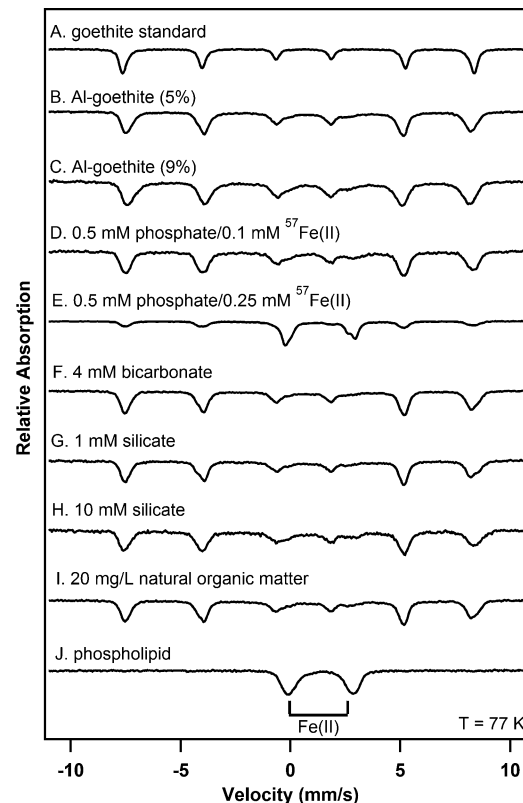


Figure 1. ⁵⁷Fe Mössbauer spectra of ⁵⁷Fe(II) reacted with ⁵⁶Fe goethites. (A) Naturally abundant Fe goethite standard, (B) ⁵⁶Fe goethite containing 5% Al-substitution and 1 mM Fe(II), (C) ⁵⁶Fe goethite containing 9% Al-substitution and 1 mM Fe(II), (D) 0.5 mM phosphate and 0.1 mM ⁵⁷Fe(II), (E) 0.5 mM phosphate and 0.25 mM Fe(II), (F) 4 mM bicarbonate and 1 mM ⁵⁷Fe(II), (G) 1 mM silicate and 1 mM ⁵⁷Fe(II), (H) 10 mM silicate and 1 mM ⁵⁷Fe(II), (I) 20 mg/L natural organic matter and 1 mM ⁵⁷Fe(II), and (J) ~1 mM 1,2-dioleoyl-sn-glycero-3-phosphatidic acid (DOPA) phospholipid + 1 mM Fe(II). Al-goethite samples were reacted for 20 h and samples with anions were reacted for 4–8 h.

sorbed $^{57}\text{Fe}(\text{II})$ has been oxidized (Figure 1B,C). A small Fe(II) doublet is present but accounts for less than 10% of the spectral area (SI Table S3). Complete dissolution of the Al-goethite suspensions by HCl resulted in Fe(II) recoveries averaging $99.3 \pm 5.4\%$ (1σ). Complete recovery of Fe(II) in the reactor indicates that no net oxidation of Fe(II) occurred and is consistent with oxidation of sorbed Fe(II) by structural Fe(III) in Al-goethite, similar to previous findings of oxidation of sorbed Fe(II) by structural Fe(III) in goethite.^{15,17,52}

While the Mössbauer spectra clearly indicate oxidation of sorbed $^{57}\text{Fe}(\text{II})$ after reaction with Al-goethite, attempts to deconvolute the spectra revealed significant complexities that are difficult to interpret and suggest that the newly formed goethite is altered from bulk goethite. The first complexity is the presence of a broad, partially ordered or collapsed feature that comprised ~20% of the area for both Al-goethite, as well as the nonsubstituted goethite. Looking back closely at our and others' previous work with goethite and $^{57}\text{Fe}(\text{II})$, we do see clear evidence of this broad feature in Amstaetter et al.²⁷ and some slight indication of it in our 2009 paper with microgoethite rods.⁵² In our 2004 paper,¹⁵ we see little indication of this type of broad feature which may be due to lower Fe(II)/Fe(III) ratio in our 2004 work compared to others.²⁷ We note that reactors with 3 mM Fe(II) had higher relative areas of the collapsed feature (~30%, SI Table S3). The lack of significant features of this broad component (even at temperatures as low as 15 K—data not shown) limits our ability to interpret this phase much beyond that it is Fe(III). We note, however, that similar collapsed features have been reported for superparamagnetic goethites with small particle size, Al-substitution, and/or poor crystallinity.^{56,57}

The second complex feature we observed was asymmetry of the goethite peaks. Goethite has an ideal ratio of relative areas between the six peaks of 3:2:1:1:2:3 as is observed for Al-goethite (Figure 2, top spectrum) and goethite (SI Figure S1, top spectrum). To account for the asymmetry, two sextets are required to adequately model the spectra (note if we were to relax the ideal ratio constraint in the model and let it float, one sextet would provide an equally adequate fit). While the first sextet has Mössbauer parameters that are generally consistent with goethite or Al-substituted goethite (SI Table S3),^{58–60} the second sextet has Mössbauer parameters that are markedly different than goethite and are closer to those for lepidocrocite. Lepidocrocite, however, has a Néel temperature near or lower than 77 K and is unlikely to be magnetically ordered at this temperature (and at higher temperatures – data not shown).^{34,61}

Again, looking back closely at our and other's previous work with goethite reacted with $^{57}\text{Fe}(\text{II})$, we do see indications of this asymmetry in the Fe(III) sextets in our previous experiments with both goethite micro- and nanorods reacted with $^{57}\text{Fe}(\text{II})$,^{15,52} as well as in both Amstaetter et al.²⁷ and Silvester et al.¹⁷ Similar to our approach, Silvester et al. fit the asymmetry of their Mössbauer data with three sextets, and attributed them to a goethite coating formed from electron transfer. It appears that this asymmetry in Fe(III) sextets for goethite formed by reacting $^{57}\text{Fe}(\text{II})$ with goethite has been observed over a range of conditions, including varying Fe(II)/Fe(III) loadings, pH, and goethite composition. The observed asymmetry in the two sextets could be due to artifacts arising from the orientation of the sample during filtering⁶² or, more interestingly, the presence of two magnetically ordered sites in goethite is reminiscent of spectra obtained in the presence of an

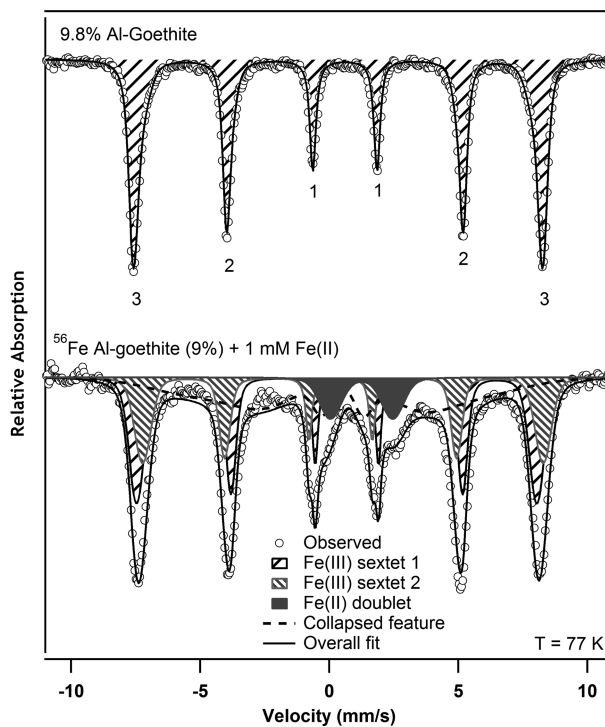


Figure 2. Mössbauer spectra of unreacted naturally abundant Al-goethite with 9.8% Al-substitution (top spectrum) and ⁵⁶Fe-goethite with 9% Al-substitution reacted with 1 mM $^{57}\text{Fe}(\text{II})$ (bottom spectrum). Unreacted goethite (top spectrum) with 9.8% Al-substitution was fit with only one sextet. The bottom spectrum was fit with two Fe(III) sextets (black and gray hatched components), an Fe(II) doublet (solid gray), and a poorly resolved collapsed feature (dashed line). Parameters from fitting are reported in SI Table S3.

applied magnetic field,^{60,62} possibly indicating some alteration in the magnetic properties of the newly formed goethite, analogous to what we previously observed for hematite.^{16,20} It is important to note that while spectra of the goethite formed from sorption-induced interfacial electron transfer are complex, having both a broad, collapsed feature, as well as an asymmetry that requires two sextets, the spectra unambiguously show that substitution of up to approximately 10% of the Fe in goethite by Al does not significantly inhibit the transfer of electrons from sorbed Fe(II) to Fe(III) in goethite.

Influence of Anion Sorption on Fe(II)-Goethite Electron Transfer. Previous work demonstrating electron transfer between Fe(II) and goethite was done under relatively simple solution conditions with only a Good's buffer and electrolyte present and it is unclear whether common groundwater anions, such as phosphate, bicarbonate, and natural organic matter will inhibit electron transfer. To address this question, we investigated electron transfer between $^{57}\text{Fe}(\text{II})$ and ⁵⁶Fe goethite in the presence of bicarbonate (4 mM HCO_3^-), silicate (1 and 10 mM SiO_4^{4-}), and natural organic matter (20 mg/L Aldrich humic acid (NOM)). Experimental conditions for each anion experiment are listed in SI Table S2. We chose a near-neutral pH for the anion experiments to favor anion sorption^{38–40} while attempting to maintain solution conditions below the solubility limit of the various Fe(II)-anion precipitates, such as siderite and vivianite.

The Mössbauer spectra shown in Figure 1-D through I indicate that electron transfer occurs between $^{57}\text{Fe}(\text{II})$ and ⁵⁶Fe goethite in the presence of 4 mM bicarbonate, 1 and 10 mM

Table 1. Mass and Fe Isotope Data for Fe Isotope Tracer Experiments between Aqueous Fe(II) and Goethite, Al-Goethite, And Goethite with Sorbed Phosphate

time (d)	aqueous Fe(II)			solids		
	Fe (μ moles)	$\delta^{57}\text{Fe}$	% exchange ^a	Fe (μ moles)	$\delta^{57}\text{Fe}$	% exchange ^{a,b}
Goethite (2 g/L) + 1 mM Fe(II)						
0	16.4 (0.312) ^c	0.968 (0.0028) ^c	0 (0) ^c	380 (4.40) ^c	0.024 (0.0000) ^c	0 (0) ^c
0.007	12.7 (0.292)	0.762 (0.0131)	22.8 (1.4)	360 (2.54)	0.043 (0.0002)	49.8 (0.49)
0.083	12.7 (0.543)	0.682 (0.0079)	31.6 (0.8)	350 (27.7)	0.045 (0.0032)	54.5 (7.9)
0.625	10.9 (2.00)	0.582 (0.0116)	42.6 (1.5)	332 (7.25)	0.053 (0.0023)	74.4 (5.8)
1.6	10.5 (4.53)	0.571 (0.0147)	43.9 (1.7)	324 (10.7)	0.056 (0.0050)	80.4 (12)
3.0	12.3 (0.516)	0.478 (0.0774)	54.2 (8.6)	315 (10.7)	0.053 (0.0009)	73.3 (2.3)
6.0	12.2 (0.643)	0.529 (0.0008)	48.5 (0.07)	332 (12.0)	0.053 (0.0016)	74.3 (4.0)
14.2	11.2 (1.06)	0.539 (0.0360)	47.4 (3.9)	308 (2.88)	0.056 (0.0004)	81.0 (5.7)
31.25	11.9 (0.464)	0.583 (0.0137)	42.6 (1.3)	332 (13.3)	0.058 (0.0005)	86.7 (2.8)
Al-Goethite (2 g/L) + 1 mM Fe(II)						
0	14.1 (0.155)	0.968 (0.0041)	0 (0)	299 (14.4)	0.024 (0.0003)	0 (0)
0.021	12.2 (0.298)	0.941 (0.0242)	2.9 (2.3)	275 (6.55)	0.030 (0.0009)	14.7 (1.1)
0.083	11.9 (0.125)	0.903 (0.0408)	6.4 (4.1)	248 (29.6)	0.031 (0.0004)	17.4 (1.0)
0.667	11.7 (0.119)	0.909 (0.0127)	6.4 (1.4)	274 (5.00)	0.033 (0.0000)	22.8 (0.4)
1.5	11.2 (0.711)	0.926 (0.0015)	4.6 (0.5)	290 (11.9)	0.034 (0.0001)	24.8 (0.5)
3.0	10.5 (0.094)	0.918 (0.0018)	5.5 (0.6)	258 (3.20)	0.036 (0.0008)	28.9 (1.3)
6.1	11.3 (0.302)	0.908 (0.0185)	6.9 (1.7)	245 (11.8)	0.036 (0.0011)	27.9 (2.4)
14.7	6.76 (0.760)	0.851 (0.0728)	12.1 (8.1)	263 (3.49)	0.044 (0.048)	46.8 (8.1)
31.1	10.5 (0.211)	0.888 (0.0196)	8.8 (2.3)	269 (8.91)	0.037 (0.0005)	31.6 (1.3)
Nanogoethite (1 g/L) + 0.1 mM Fe(II)						
0	1.723 (0.010)	0.906 (0.027)	0.0 (0.0)	125 (4.4)	0.024 (0.001)	0 (0)
0.007	0.188 (0.016)	0.604 (0.008)	34.7 (0.8)	120 (0.7)	0.038 (0.000)	131 (0.065)
3	0.126 (0.023)	0.340 (0.026)	64.9 (3.0)	119 (1.3)	0.035 (0.001)	104 (0.015)
10	0.129 (0.024)	0.099 (0.021)	92.5 (2.4)	120 (0.2)	0.035 (0.000)	108 (0.054)
16	0.129 (0.040)	0.086 (0.008)	94.1 (0.8)	118 (1.0)	0.035 (0.000)	108 (0.04)
21	0.146 (0.020)	0.084 (0.001)	94.3 (0.2)	118 (0.8)	0.035 (0.001)	107 (0.04)
Nanogoethite (1 g/L) + 0.35 mM PO ₄ + 0.1 mM Fe(II)						
0	1.723 (0.010)	0.906 (0.027)	0.0 (0.0)	150 (5.3)	0.024 (0.000)	0 (0)
0.007	0.111 (0.012)	0.706 (0.066)	23.0 (7.5)	142 (6.2)	0.031 (0.003)	68.8 (0.24)
0.5	0.080 (0.014)	0.255 (0.071)	74.7 (8.1)	138 (1.0)	0.034 (0.001)	92.4 (0.049)
1	0.081 (0.051)	0.187 (0.031)	82.5 (3.5)	138 (4.2)	0.035 (0.004)	101 (0.46)
3	0.139 (0.011)	0.141 (0.034)	87.7 (3.9)	138 (3.5)	0.036 (0.001)	120 (0.13)
10	0.143 (0.030)	0.080 (0.021)	94.7 (2.4)	139 (4.1)	0.036 (0.003)	111 (2.9)
16	0.162 (0.042)	0.047 (0.018)	98.6 (2.1)	139 (3.1)	0.036 (0.007)	112 (0.86)
21	0.157 (0.013)	0.039 (0.011)	99.4 (1.2)	141 (5.1)	0.035 (0.000)	110 (0.04)

^a% exchange calculated using eq 2 in the text. ^bThe % exchange calculated from the solids is initially biased by sorption of isotopically heavy ^{57}Fe from solution. ^cStandard deviation measured from triplicate reactors.

silicate, and NOM. In general, except for Figure 1-E (discussed below), these spectra are all similar to the spectrum collected with 1 mM $^{57}\text{Fe}(\text{II})$ in the absence of anions, as well as with the Al-substituted goethite (Figure 2). The spectra contain the broad collapsed feature, an asymmetry that requires two sextets to fit, and a small Fe(II) doublet. A detailed spectral fitting for goethite reacted with phosphate and $^{57}\text{Fe}(\text{II})$ is provided in SI Figure S5 and Table S3, as an example. In all cases, the results of the experiments indicate that electron transfer occurs between sorbed Fe(II) and goethite resulting in formation of goethite that is altered from bulk goethite (i.e., has the broad, collapsed feature and asymmetry). Interestingly, previous results showed that both silicate and NOM decrease the rate and extent of isotope exchange between Fe(II) and Fe(III) oxides.^{12,31} Our observation that electron transfer occurs in the presence of both silicate and NOM suggests a lack of electron transfer at the surface is probably not the limiting factor in those experiments, but rather another process, such as reductive

detachment of Fe(II) from the solid that may have limited the rate and extent of Fe atom exchange.

We were also particularly interested in whether phosphate would influence electron transfer between Fe(II) and goethite given the extensive sorption of phosphate on goethite and the role of phosphate in the transformation of Fe oxide (e.g., refs 34,48, and 63). We chose conditions to provide enough Fe(II) to see in the Mössbauer spectra and enough phosphate to achieve full surface coverage (SI Figure S6). We used 0.5 mM phosphate at two Fe(II) loadings—0.125 and 0.25 mM—and in both experiments the total Fe(II) and phosphate concentrations exceed the solubility of vivianite ($\text{Fe}_3(\text{PO}_4)_2 \cdot 8\text{H}_2\text{O}$, $\text{pK}_{\text{sp}} = 33.04$).⁶⁴ Despite the supersaturation of vivianite in both experiments, the Mössbauer spectra (Figure 1-D and E) indicate that electrons have been transferred from Fe(II) to the underlying goethite to form an altered goethite coating with similar broad, collapsed and asymmetric features as observed with Al-goethite and carbonate, silicate and NOM (SI Figure S5 and Table S3). A minor amount of vivianite is

observed in the spectra at the lower Fe(II) loading (<10%, Figure 1-D), whereas, in the higher Fe(II) loading experiment (Figure 1-E) vivianite comprises ~60% of the spectral area (SI Table S3). In both cases, however, there is still clear indication that a goethite coating has formed from oxidation of Fe(II) by Fe(III) in goethite.

Influence of Phospholipid Sorption on Fe(II)-Goethite

Electron Transfer. In order to explore the possible influence of biological materials on electron transfer (and, frankly, to get something to inhibit electron transfer!), we also investigated the effect of sorbed phospholipids on electron transfer between ^{57}Fe (II) and ^{56}Fe goethite. Phospholipids are biomolecules that make up the cell membranes in living organisms, and have recently been shown to form supported bilayers and multilayers on metal oxide particles.⁶⁵ We exposed ^{56}Fe goethite to approximately 1 mM 1,2-dioleoyl-sn-glycero-3-phosphate (DOPA) and then reacted it with ^{57}Fe (II). As anticipated based on the potential electron donor-electron acceptor separation of approximately 5 nm,^{66,67} the Mössbauer spectrum indicates the presence of only Fe(II) as an Fe(II) doublet, indicating that electron transfer between ^{57}Fe (II) and ^{56}Fe goethite does *not* occur in the presence this long-chain (C18) phospholipid and suggests that the presence of large concentrations of biomass may inhibit Fe(II)-Fe(III) oxide electron transfer.

Influence of Al-Substitution and Phosphate on Goethite Fe Atom Exchange. Having demonstrated that electron transfer occurs between aqueous Fe(II) and Fe(III) in Al-substituted goethite and in the presence of several common groundwater anions, we were interested whether Al-substitution or anion sorption influences the rate and extent of isotope exchange between aqueous Fe(II) and goethite. Several previous studies have shown that Al-substitution can decrease the rate of iron oxide reductive dissolution both by chemical^{4,35} and biological reductants,^{36,37} and hinder the crystallization of ferrihydrite to more stable oxides.⁶⁸ We hypothesized that incorporation of redox-inactive Al(III) into goethite might inhibit atom exchange between aqueous Fe(II) and goethite by blocking reductive dissolution of Fe from Al-goethite, or perhaps through inhibition of bulk electron conduction.

To track redox induced atom exchange between Fe(II) and Al-substituted goethite, we reacted an enriched ^{57}Fe (II) isotope tracer (96.8% ^{57}Fe) with a suspension of 10% Al-substituted goethite having a natural isotope composition (2.4% ^{57}Fe) and tracked the change in the isotope composition of the aqueous and solid phases with time (Figure 3A). For comparison, we used a goethite control synthesized in 0.3 M KOH aged at 70 °C for 72 h, longer than the typical 60 h, at a pH where goethite crystallization is rapid.^{50,51} The resulting goethite control has a particle size ($l \times w$) of $(1090 \pm 740) \times (166 \pm 91)$ nm which is similar in width but longer in length than the Al-goethite $(416 \pm 153) \times (158 \pm 99)$ nm (SI Figure S3, Table S1). In the aluminum-free goethite control, the fraction of the total ^{57}Fe ($f^{57}\text{Fe} = ^{57}\text{Fe}/\Sigma\text{Fe}$) in the aqueous phase decreases substantially over the first day while the fraction in the solid phase increases (solids + Fe(II) taken up by the solids) (Figure 3A and Table 1), indicating Fe atom exchange has occurred. In comparison, both the solid and aqueous phase in the Al-goethite showed only small changes in $f^{57}\text{Fe}$. In contrast to our previous work with goethite nanorods,¹⁸ neither the goethite control nor the Al-goethite reached the calculated mass-balance for isotopic equilibrium ($f^{57}\text{Fe}_{\text{goethite},e} = 0.0634$, $f^{57}\text{Fe}_{\text{Al-goethite},e} = 0.0660$) after 30 days, suggesting that only a portion of the Fe

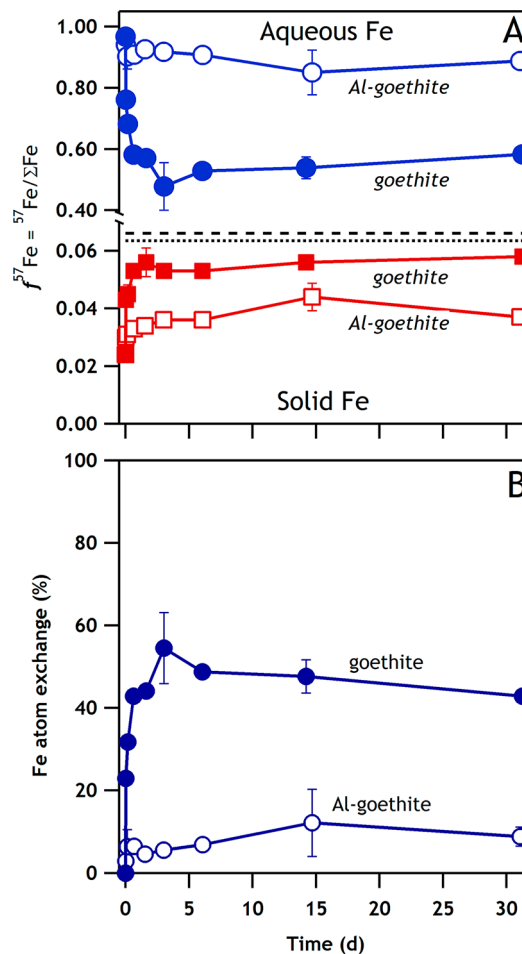


Figure 3. Effect of Al-substitution on isotope exchange between an enriched aqueous ^{57}Fe (II) tracer and 2 g L⁻¹ Al-free goethite (closed markers) or 10% Al-substituted goethite (open markers). (A) Measured $^{57}\text{Fe}/\Sigma\text{Fe}$ data for aqueous Fe(II) and goethite solids + Fe(II) taken up by the solids. (B) Calculated isotope exchange using data from (A) and eq 2. The dashed and dotted lines indicate the calculated mass balance on ^{57}Fe for Al-goethite (0.0660) and the dotted line for the Al-free goethite control ($f^{57}\text{Fe} = 0.0634$), respectively. Error bars represent one standard deviation.

atoms in goethite exchanged with aqueous Fe(II). To quantify the extent of Fe atom exchange between the aqueous Fe(II) and goethite solids, we used:^{31,69}

$$\text{percent exchange} = \frac{f_t - f_i}{f_e - f_i} \times 100 \quad (2)$$

Here, f_t is the isotopic composition (as measured by $f^{57}\text{Fe} = ^{57}\text{Fe}/\Sigma\text{Fe}$) at time t , f_i is the initial isotopic composition, and f_e is the equilibrium isotopic composition of the phase of interest.⁶⁹ As we noted previously, sorption of ^{57}Fe (II) at the surface of the goethite biases the solid phase toward a heavier composition.²² Because of the bias in the solid-phase $f^{57}\text{Fe}$, we chose to use the aqueous phase $f^{57}\text{Fe}$ to calculate atom exchange (Figure 3B and Table 1). Rather than trying to correct for the sorption bias by extracting the sorbed Fe(II) with acid as we have in our previous work,^{18,22} we verified our atom exchange estimates calculated from the aqueous phase isotope composition by also tracking release of ^{54}Fe from the solids to the aqueous phase, as the starting aqueous phase Fe(II) is highly depleted in ^{54}Fe (<0.1%). We found excellent

agreement between the amount of exchange estimated from the depletion of aqueous ^{57}Fe and the increase of aqueous ^{54}Fe atom (within 1%) (SI Table S4).

Calculation of the amount of atom exchange between Fe(II) and Al-goethite indicates that approximately 12% exchange between the aqueous Fe(II) and the Al-goethite solids occurred, which is substantially less than the 43% observed for the goethite control (Figure 3B). The difference between the goethite control and the Al-goethite suggests that structural Al-substitution in goethite may be inhibiting atom exchange between aqueous Fe(II) and solid Fe(III). Previously, we proposed a “redox-driven conveyor belt” model that includes sorption of aqueous Fe(II), $\text{Fe}(\text{II})_{\text{aq}}-\text{Fe}(\text{III})_{\text{oxide}}$ electron transfer, bulk conduction, and reductive dissolution of the goethite to explain the near complete atom exchange we observed between Fe(II) and goethite nanorods.¹⁸ Based on the Mössbauer results described above, it is clear that $\text{Fe}(\text{II})_{\text{aq}}-\text{Fe}(\text{III})_{\text{oxide}}$ electron transfer still occurs with Al-goethite indicating that the electron transfer step is unlikely to be responsible for the decreased extent of atom exchange in Al-goethite.

At this point, we can only speculate on the potential cause of decreased atom exchange in the Al-goethite. One possibility is that the decreased atom exchange for Al-goethite has little to do with the presence of Al, but is simply due to particle size or crystallinity differences, as it is difficult to keep these constant between the different synthesis methods needed for Al-goethite and goethite. The Al-goethite used here were about the same width, but longer than the Al-free goethite (Al-goethite: 416×158 nm; goethite: 1090×166 nm; (SI Table S1). Conversely, pXRD determined mean crystallite dimensions (MCD) indicate that the Al-goethite is more crystalline than the Al-free goethite (SI Table S1). More interestingly, however, is the possibility that Fe atom exchange is decreased in Al-goethite due to either inhibition of reductive dissolution of the Al-goethite, formation of an Al coating during Fe(II) induced dissolution, or reduced conductivity in the bulk mineral. Previous studies have shown that the presence structural or adsorbed Al reduces the rate and/or extent of Fe oxide dissolution by chemical reductants and metal reducing bacteria, possibly through blocking by an Al-coating.^{4,35–37} Both incorporated and sorbed Al have been shown to slow the transformation of ferrihydrite to more crystalline Fe oxides, presumably through decreased dissolution of the Al-ferrihydrite.⁶⁸ As for conductivity, while we cannot rule it out, we note that up to 5% Al-substitution has been shown to have no effect on goethite conductivity,⁷⁰ and it has been suggested, based on percolation theory, that at least 10% substitution is needed to significantly inhibit electron hopping.⁷¹ Note that we observed less atom exchange with our Al-free goethite particles here compared to the complete exchange with Al-free goethite nanorods (81×11 nm) in our previous work.¹⁸ We speculate that this may be due to the significant differences in particle sizes, and additional studies are underway to evaluate the influence of particle size on Fe atom exchange between aqueous Fe(II) and Fe(III) oxides.

In addition to Al-substitution, we also evaluated whether phosphate influences atom exchange between Fe(II) and goethite. We hypothesized that phosphate would inhibit Fe atom exchange since phosphate is known to inhibit Fe-mineral recrystallization and change the distribution of Fe-products during reduction or oxidation.^{48,63,72–74} We used nanogoethite particles because we have previously observed more extensive

exchange with smaller particles.¹⁸ We chose conditions to (i) avoid precipitation of vivianite, (ii) increase the ^{57}Fe mass to be able to detect changes in the solid ^{57}Fe content, and (iii) achieve approximately a monolayer coverage of phosphate on goethite (SI Figure S6). We observed no significant influence of phosphate on the rate or extent of Fe atom exchange (Figure 4). Near-complete exchange was observed in the presence and

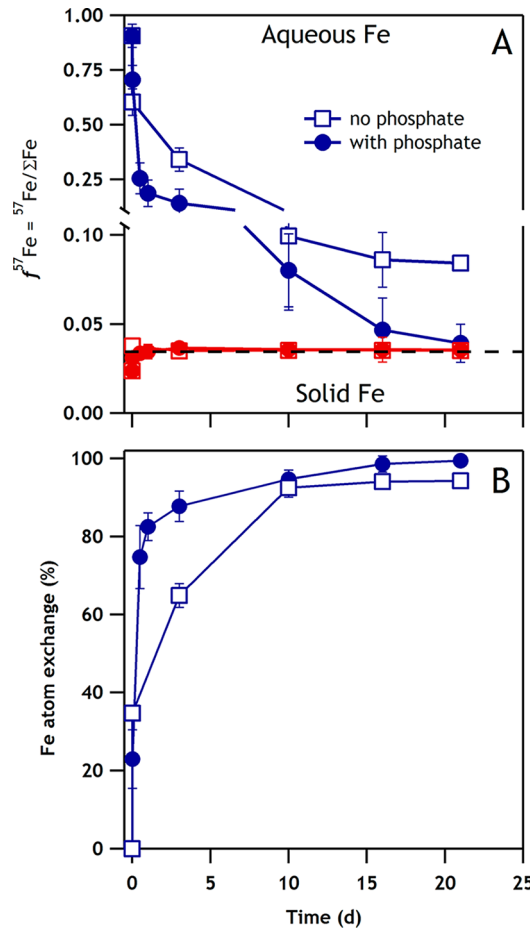


Figure 4. Effect of phosphate on isotope exchange between 0.1 mM aqueous Fe(II) and 1 g L^{-1} nanogoethite with and without 0.35 mM sorbed phosphate. (A) Measured $^{57}\text{Fe}/\Sigma\text{Fe}$ data for aqueous Fe(II) and goethite solids + Fe(II) taken up by the solids. The dashed line indicates the calculated mass balance on ^{57}Fe ($f^{57}\text{Fe} = 0.0344$). (B) Percent exchange of ^{57}Fe between aqueous Fe(II) and goethite. Error bars represent one standard deviation.

absence of phosphate (94 and 99%, respectively). Our observations suggest that sorbed phosphate has little effect on both electron transfer and atom exchange between aqueous Fe(II) and goethite, which is somewhat surprising given that phosphate is well-known to influence Fe product formation during Fe(II) oxidation, Fe(II)-Fe(III) coprecipitation, and dissimilatory Fe(III) reduction.^{48,63,72–74}

Environmental Implications. Our results show that electron transfer occurs between aqueous Fe(II) and structural Fe(III) in goethite occur over a range of conditions, including structural Al-for-Fe substitution and in the presence of environmentally relevant concentrations of common anions. We further show that Fe atom exchange is unaffected by phosphate sorption, but may be inhibited by Al-substitution. Atom exchange between aqueous Fe(II) and goethite has been

hypothesized to (i) catalyze the incorporation of metals from solution into the structure of the oxide, or (ii) catalyze the release of incorporated metals from the structure of oxide to solution.^{18,23–25} Recent studies suggest that redox-driven incorporation and release of elements from goethite depend on the properties of the trace element, with divalent metals like Ni, Co, and Zn undergoing release and incorporation during atom exchange, whereas AsO₄³⁻ only sorbed or precipitated with Fe(II).^{22,23,37S} Our work suggests that Al-substitution may decrease the amount of trace-metal cycling that occurs between Fe(II) and Fe oxides.⁷⁶ Questions remain regarding the mechanisms by which anions influence electron transfer and atom exchange between Fe(II) and Fe(III) oxides, such as, why we observed no inhibition of either process by phosphate, and saw no effect of silicate on electron transfer, but others have seen decreased atom exchange in the presence of silicate.^{12,30,31} Our work provides evidence which suggests that the electron transfer step may not be limiting in cases where decreased isotope exchange is observed. Finally, given the lack of observed electron transfer between Fe(II) and goethite in the presence of a sorbed phospholipid, we speculate that atom exchange and concomitant trace metals release may be inhibited at high biomass loadings, such as those that develop during engineered biostimulation experiments.

ASSOCIATED CONTENT

Supporting Information

As mentioned in the text, additional text, tables and figures are available. This material is available free of charge via the Internet at <http://pubs.acs.org>.

AUTHOR INFORMATION

Corresponding Author

*Phone: (630)252-3985; e-mail: dlatta@anl.gov.

Present Address

[†]Biosciences Division, Argonne National Laboratory, Argonne, Illinois, 60439, United States.

Notes

The authors declare no competing financial interest.

ACKNOWLEDGMENTS

We gratefully acknowledge J. Thompson for his help and suggestions with operating the ICP-MS. We also thank M. St. Clair, C. A. Gorski, R. M. Handler, and M. V. Schaefer for helpful discussions during the course of this work. We acknowledge The University of Iowa Central Microscopy facility for use of microscopy resources. Comments from three anonymous reviewers helped improve this manuscript. Funding for this work was provided from the National Science Foundation (NSF) through Grant No. CHE-1012037 and EAR-0821615 and through the Subsurface Science Scientific Focus Area (SFA) at Argonne National Laboratory (ANL) supported by the Subsurface Biogeochemical Research Program, Office of the Biological and Environmental Research, Office of Science, U.S. Department of Energy (DOE), under contract DE-AC02-06CH11357.

REFERENCES

- Lipson, D. A.; Jha, M.; Raab, T. K.; Oechel, W. C. Reduction of iron (III) and humic substances plays a major role in anaerobic respiration in an Arctic peat soil. *J. Geophys. Res. [Biogeosci.]* **2010**, 115.
- Lloyd, J. R. Microbial reduction of metals and radionuclides. *Fems Microbiology Reviews* **2003**, 27 (2–3), 411–425.
- Lack, J. G.; Chaudhuri, S. K.; Chakraborty, R.; Achenbach, L. A.; Coates, J. D. Anaerobic biooxidation of Fe(II) by *Dechlorosoma sullum*. *Microbial Ecology* **2002**, 43 (4), 424–431.
- Murray, G. C.; Hesterberg, D. Iron and phosphate dissolution during abiotic reduction of ferrihydrite-boehmite mixtures. *Soil Sci. Soc. Am. J.* **2006**, 70 (4), 1318–1327.
- Posth, N. R.; Hegler, F.; Konhauser, K. O.; Kappler, A. Alternating Si and Fe deposition caused by temperature fluctuations in Precambrian oceans. *Nat. Geosci.* **2008**, 1 (10), 703–708.
- Schaetzl, R.; Anderson, S. *Soils: Genesis and Geomorphology*; Cambridge University Press: Cambridge, UK, 2005; p 817.
- Klausen, J.; Trober, S. P.; Haderlein, S. B.; Schwarzenbach, R. P. Reduction of substituted nitrobenzenes by Fe(II) in aqueous mineral suspensions. *Environ. Sci. Technol.* **1995**, 29 (9), 2396–2404.
- Charlet, L.; Silvester, E.; Liger, E. N-compound reduction and actinide immobilisation in surficial fluids by Fe(II): The surface Fe(III)OFe(II)OH degrees species, as major reductant. *Chem. Geol.* **1998**, 151 (1–4), 85–93.
- Tamura, Y.; Saturno, M.; Yamada, K.; Katsura, T. The transformation of γ-FeOOH to Fe₃O₄ and green rust II in an aqueous solution. *Bull. Chem. Soc. Jpn.* **1984**, 57 (9), 2417–2421.
- Hansel, C. M.; Benner, S. G.; Fendorf, S. Competing Fe(II)-induced mineralization pathways of ferrihydrite. *Environ. Sci. Technol.* **2005**, 39, 7147–7153.
- Pedersen, H. D.; Postma, D.; Jakobsen, R.; Larsen, O. Fast transformation of iron oxyhydroxides by the catalytic action of aqueous Fe(II). *Geochim. Cosmochim. Acta* **2005**, 69 (16), 3967–3977.
- Jones, A. M.; Collins, R. N.; Rose, J.; Waite, T. D. The effect of silica and natural organic matter on the Fe(II)-catalysed transformation and reactivity of Fe(III) minerals. *Geochim. Cosmochim. Acta* **2009**, 73 (15), 4409–4422.
- Burton, E. D.; Johnston, S. G.; Watling, K.; Bush, R. T.; Keene, A. F.; Sullivan, L. A. Arsenic effects and behavior in association with the Fe(II)-catalyzed transformation of schwertmannite. *Environ. Sci. Technol.* **2010**, 44 (6), 2016–2021.
- Coughlin, B. R.; Stone, A. T. Nonreversible adsorption of divalent metal-ions (Mn^{II}, Co^{II}, Ni^{II}, Cu^{II}, and Pb^{II}) onto goethite—Effects of acidification, Fe^{II} addition, and picolinic-acid addition. *Environ. Sci. Technol.* **1995**, 29 (9), 2445–2455.
- Williams, A. G. B.; Scherer, M. M. Spectroscopic evidence for Fe(II)-Fe(III) electron transfer at the Fe oxide-water interface. *Environ. Sci. Technol.* **2004**, 38 (18), 4782–4790.
- Larese-Casanova, P.; Scherer, M. M. Fe(II) sorption on hematite: New insights based on spectroscopic measurements. *Environ. Sci. Technol.* **2007**, 41 (2), 471–477.
- Silvester, E.; Charlet, L.; Tournassat, C.; Gehin, A.; Grenache, J.-M.; Liger, E. Redox potential measurements and Mössbauer spectrometry of Fe^{II} adsorbed onto Fe^{III} (oxyhydr)oxides. *Geochim. Cosmochim. Acta* **2005**, 69 (20), 4801–4815.
- Handler, R. M.; Beard, B. L.; Johnson, C. M.; Scherer, M. M. Atom exchange between aqueous Fe(II) and goethite: An Fe isotope tracer study. *Environ. Sci. Technol.* **2009**, 43 (4), 1102–1107.
- Yanina, S. V.; Rosso, K. M. Linked Reactivity at mineral-water interfaces through bulk crystal conduction. *Science* **2008**, 320 (5873), 218–222.
- Rosso, K. M.; Yanina, S. V.; Gorski, C. A.; Larese-Casanova, P.; Scherer, M. M. Connecting observations of hematite (α -Fe₂O₃) growth catalyzed by Fe(II). *Environ. Sci. Technol.* **2010**, 44 (1), 61–67.
- Gorski Christopher, A.; Scherer, M. M. Fe²⁺ sorption at the Fe oxide-water interface: A revised conceptual framework. In *Aquatic Redox Chemistry*; American Chemical Society: 2011; Vol. 1071, pp 315–343.
- Gorski, C. A.; Handler, R. M.; Beard, B. L.; Pasakarnis, T.; Johnson, C. M.; Scherer, M. M. Fe atom exchange between aqueous Fe²⁺ and magnetite. *Environ. Sci. Technol.* **2012**.

- (23) Frierdich, A. J.; Catalano, J. G. Controls on Fe(II)-activated trace element release from goethite and hematite. *Environ. Sci. Technol.* **2012**, *46* (3), 1519–1526.
- (24) Frierdich, A. J.; Luo, Y.; Catalano, J. G. Trace element cycling through iron oxide minerals during redox driven dynamic recrystallization. *Geology* **2011**.
- (25) Boland, D. D.; Collins, R. N.; Payne, T. E.; Waite, T. D. Effect of amorphous Fe(III) oxide transformation on the Fe(II)-Mediated Reduction of U(VI). *Environ. Sci. Technol.* **2011**, *45* (4), 1327–1333.
- (26) Pedersen, H. D.; Postma, D.; Jakobsen, R. Release of arsenic associated with the reduction and transformation of iron oxides. *Geochim. Cosmochim. Acta* **2006**, *70* (16), 4116–4129.
- (27) Amstaetter, K.; Borch, T.; Larese-Casanova, P.; Kappler, A. Redox transformation of arsenic by Fe(II)-activated goethite (α -FeOOH). *Environ. Sci. Technol.* **2009**, *44* (1), 102–108.
- (28) Hiemstra, T.; van Riemsdijk, W. H. Adsorption and surface oxidation of Fe(II) on metal (hydr)oxides. *Geochim. Cosmochim. Acta* **2007**, *71* (24), 5913–5933.
- (29) Collins, R. N.; Waite, T. D. Isotopically exchangeable concentrations of elements having multiple oxidation states: The case of Fe(II)/Fe(III) isotope self-exchange in coastal lowland acid sulfate soils. *Environ. Sci. Technol.* **2009**, *43* (14), 5365–5370.
- (30) Wu, L.; Percak-Dennett, E. M.; Beard, B. L.; Roden, E. E.; Johnson, C. M. Stable iron isotope fractionation between aqueous Fe(II) and model Archean ocean Fe–Si coprecipitates and implications for iron isotope variations in the ancient rock record. *Geochim. Cosmochim. Acta* **2012**, *84* (0), 14–28.
- (31) Wu, L.; Beard, B. L.; Roden, E. E.; Johnson, C. M. Stable iron isotope fractionation between aqueous Fe(II) and hydrous ferric oxide. *Environ. Sci. Technol.* **2011**, *45* (5), 1847–1852.
- (32) Wu, L. L.; Beard, B. L.; Roden, E. E.; Kennedy, C. B.; Johnson, C. M. Stable Fe isotope fractionations produced by aqueous Fe(II)-hematite surface interactions. *Geochim. Cosmochim. Acta* **2010**, *74* (15), 4249–4265.
- (33) Norrish, K.; Taylor, R. M. Isomorphous replacement of iron by aluminium in soil goethites. *J. Soil Sci.* **1961**, *12* (2), 294–&.
- (34) Cornell, R. M.; Schwertmann, U. *The Iron Oxides: Structure, Properties, Reactions, Occurrences and Uses*, 2nd ed.; Wiley-VCH: Weinheim, Germany, 2003; p 664.
- (35) Torrent, J.; Schwertmann, U.; Barron, V. The reductive dissolution of synthetic goethite and hematite in dithionite. *Clay Minerals* **1987**, *22* (3), 329–337.
- (36) Dominik, P.; Pohl, H. N.; Bousserrhine, N.; Berthelin, J.; Kaupenjohann, M. Limitations to the reductive dissolution of Al-substituted goethites by *Clostridium butyricum*. *Soil Biology & Biochemistry* **2002**, *34* (8), 1147–1155.
- (37) Ekstrom, E. B.; Learman, D. R.; Madden, A. S.; Hansel, C. M. Contrasting effects of Al substitution on microbial reduction of Fe(III) (hydr)oxides. *Geochim. Cosmochim. Acta* **2010**, *74* (24), 7086–7099.
- (38) Weng, L. P.; Van Riemsdijk, W. H.; Koopal, L. K.; Hiemstra, T. Adsorption of humic substances on goethite: Comparison between humic acids and fulvic acids. *Environ. Sci. Technol.* **2006**, *40* (24), 7494–7500.
- (39) Villalobos, M.; Trotz, M. A.; Leckie, J. O. Variability in goethite surface site density: Evidence from proton and carbonate sorption. *J. Colloid Interface Sci.* **2003**, *268* (2), 273–287.
- (40) Hiemstra, T.; Barnett, M. O.; van Riemsdijk, W. H. Interaction of silicic acid with goethite. *J. Colloid Interface Sci.* **2007**, *310* (1), 8–17.
- (41) Strauss, R.; Brummer, G. W.; Barrow, N. J. Effects of crystallinity of goethite 0.2. Rates of sorption and desorption of phosphate. *Eur. J. Soil Sci.* **1997**, *48* (1), 101–114.
- (42) Parfitt, R. L.; Atkinson, R. J. Phosphate Adsorption on goethite (α -FeOOH). *Nature* **1976**, *264* (5588), 740–742.
- (43) Stachowicz, M.; Hiemstra, T.; van Riemsdijk, W. H. Multi-competitive interaction of As(III) and As(V) oxyanions with Ca(2+), Mg(2+), PO(3-)4, and CO(2-)3 ions on goethite. *J. Colloid Interface Sci.* **2008**, *320* (2), 400–414.
- (44) Kwon, K. D.; Kubicki, J. D. Molecular orbital theory study on surface complex structures of phosphates to iron hydroxides: Calculation of vibrational frequencies and adsorption energies. *Langmuir* **2004**, *20* (21), 9249–9254.
- (45) Persson, P.; Nilsson, N.; Sjoberg, S. Structure and bonding of orthophosphate ions at the iron oxide aqueous interface. *J. Colloid Interface Sci.* **1996**, *177* (1), 263–275.
- (46) Urrutia, M. M.; Roden, E. E.; Fredrickson, J. K.; Zachara, J. M. Microbial and surface chemistry controls on reduction of synthetic Fe(III) oxide minerals by the dissimilatory iron-reducing bacterium *Shewanella alga*. *Geomicrobiology Journal* **1998**, *15* (4), 269–291.
- (47) Borch, T.; Masue, Y.; Kukkadapu, R. K.; Fendorf, S. Phosphate imposed limitations on biological reduction and alteration of ferrihydrite. *Environ. Sci. Technol.* **2007**, *41* (1), 166–172.
- (48) O'Loughlin, E. J.; Gorski, C. A.; Scherer, M. M.; Boyanov, M. I.; Kemner, K. M. Effects of oxyanions, natural organic matter, and bacterial cell numbers on the bioreduction of lepidocrocite (γ -FeOOH) and the formation of secondary mineralization products. *Environ. Sci. Technol.* **2010**, *44* (12), 4570–4576.
- (49) Lewis, D. G.; Schwertmann, U. Influence of aluminum on the formation of iron-oxides 0.4. Influence of [Al], [OH], and temperature. *Clays Clay Miner.* **1979**, *27* (3), 195–200.
- (50) Schwertmann, U.; Cornell, R. M., *Iron Oxides in the Laboratory: Preparation and Characterization*, 2nd ed.; Wiley-VCH: New York, 2000; p 188.
- (51) Burleson, D. J.; Penn, R. L. Two-step growth of goethite from ferrihydrite. *Langmuir* **2006**, *22* (1), 402–409.
- (52) Cwiertny, D. M.; Handler, R. M.; Schaefer, M. M.; Grassian, V. H.; Scherer, M. M. Interpreting nanoscale size-effects in aggregated Fe-oxide suspensions: Reaction of Fe(II) with goethite. *Geochim. Cosmochim. Acta* **2008**, *72* (5), 1365–1380.
- (53) Clesceri, L. S.; Greenberg, A. E.; Trussell, R. R. *Standard Methods for the Examination of Water and Wastewater*, 17 ed.; American Public Health Association: Washington, DC, 1989.
- (54) Tamura, H.; Goto, K.; Yotsuyan, T.; Nagayama, M. Spectrophotometric determination of iron(II) with 1,10-phenanthroline in presence of large amounts of iron(III). *Talanta* **1974**, *21* (4), 314–318.
- (55) Murad, E.; Cashion, J. *Mössbauer Spectroscopy of Environmental Materials and their Industrial Utilization*; Kluwer Academic Publishers: Norwell, MA2004.
- (56) van der Zee, C.; Roberts, D. R.; Rancourt, D. G.; Slomp, C. P. Nanogoethite is the dominant reactive oxyhydroxide phase in lake and marine sediments. *Geology* **2003**, *31*, 993–996.
- (57) Murad, E.; Schwertmann, U. The influence of aluminum substitution and crystallinity on the Mössbauer-spectra of goethite. *Clay Minerals* **1983**, *18* (3), 301–312.
- (58) Fysh, S. A.; Clark, P. E. Aluminous goethite—A Mössbauer study. *Phys. Chem. Miner.* **1982**, *8* (4), 180–187.
- (59) Golden, D. C.; Bowen, L. H.; Weed, S. B.; Bigham, J. M. Mössbauer studies of synthetic and soil occurring aluminum-substituted goethites. *Soil Sci. Soc. Am. J.* **1979**, *43* (4), 802–808.
- (60) Pollard, R. J.; Pankhurst, Q. A.; Zientek, P. Magnetism in aluminous goethite. *Phys. Chem. Miner.* **1991**, *18* (4), 259–264.
- (61) Hirt, A. M.; Lanci, L.; Dobson, J.; Weidler, P.; Gehring, A. U. Low-temperature magnetic properties of lepidocrocite. *J. Geophys. Res.* **2002**, *107* (B1), 2011.
- (62) Forsyth, J. B.; Hedley, I. G.; Johnson, C. E. The magnetic structure and hyperfine field of goethite (α -FeOOH). *J. Phys. C: Solid State Phys.* **1968**, *1* (1), 179.
- (63) Borch, T.; Masue, Y.; Kukkadapu, R. K.; Fendorf, S. Phosphate imposed limitations on biological reduction and alteration of ferrihydrite. *Environ. Sci. Technol.* **2007**, *41*, 166–172.
- (64) Al-Borno, A.; Tomson, M. B. The temperature-dependence of the solubility product constant of vivianite. *Geochim. Cosmochim. Acta* **1994**, *58* (24), 5373–5378.
- (65) Xu, J.; Stevens, M. J.; Oleson, T. A.; Last, J. A.; Sahai, N. Role of oxide surface chemistry and phospholipid phase on adsorption and self-assembly: Isotherms and atomic force microscopy. *J. Phys. Chem. C* **2009**, *113* (6), 2187–2196.

- (66) Li, T. T.; Weaver, M. J. Intramolecular electron transfer at metal surfaces. 4. Dependence of tunneling probability upon donor-acceptor separation distance. *J. Am. Chem. Soc.* **1984**, *106*, 6107–6108.
- (67) Wigginton, N. S.; Rosso, K. M.; Stack, A. G.; Hochella, M. F. Long-range electron transfer across cytochrome-hematite (α -Fe₂O₃) interfaces. *J. Phys. Chem. C* **2009**, *113* (6), 2096–2103.
- (68) Hansel, C. M.; Learman, D. R.; Lentini, C. J.; Ekstrom, E. B. Effect of adsorbed and substituted Al on Fe(II)-induced mineralization pathways of ferrihydrite. *Geochim. Cosmochim. Acta* **2011**, *75* (16), 4653–4666.
- (69) Guilbaud, R.; Butler, I. B.; Ellam, R. M.; Rickard, D. Fe isotope exchange between Fe(II)_{aq} and nanoparticulate mackinawite (FeS_m) during nanoparticle growth. *Earth Planet. Sci. Lett.* **2010**, *300* (1–2), 174–183.
- (70) Kaneko, K.; Inoue, N.; Ishikawa, T. Electrical and photo-adsorptive properties of valence-controlled α -FeOOH. *J. Phys. Chem.* **1989**, *93* (5), 1988–1992.
- (71) Blauch, D. N.; Savéant, J.-M. Dynamics of electron hopping in assemblies of redox centers. Percolation and diffusion. *J. Am. Chem. Soc.* **1992**, *114* (9), 3323–3332.
- (72) Refait, P.; Reffass, M.; Landoulsi, J.; Sabot, R.; Jeannin, M. Role of phosphate species during the formation and transformation of the Fe(II-III) hydroxycarbonate green rust. *Colloids Surf, A* **2007**, *299* (1–3), 29–37.
- (73) Benali, O.; Abdelmoula, M.; Refait, P.; Genin, J. M. R. Effect of orthophosphate on the oxidation products of Fe(II)-Fe(III) hydroxycarbonate: The transformation of green rust to ferrihydrite. *Geochim. Cosmochim. Acta* **2001**, *65* (11), 1715–1726.
- (74) Cumplido, J.; Barron, V.; Torrent, J. Effect of phosphate on the formation of nanophase lepidocrocite from Fe(II) sulfate. *Clays Clay Miner.* **2000**, *48* (5), 503–510.
- (75) Catalano, J. G.; Luo, Y.; Otemuyiwa, B. Effect of aqueous Fe(II) on arsenate sorption on goethite and hematite. *Environ. Sci. Technol.* **2011**, *45* (20), 8826–8833.
- (76) Friedrich, A. J.; Scherer, M. M.; Bachman, J. E.; Engelhard, M. H.; Rapponetti, B. W.; Catalano, J. G. Inhibition of trace element release during Fe(II)-activated recrystallization of Al-, Cr-, and Sn-substituted goethite and hematite. *Environ. Sci. Technol.* **2012**, DOI: 10.1021/es302137d.

Supporting Information

Fe electron transfer and atom exchange in goethite: Influence of Al-substitution and anion sorption

Drew E. Latta^{1,2}, Jonathan E. Bachman¹, and Michelle M. Scherer¹*

¹*Department of Civil and Environmental Engineering, The University of Iowa, Iowa City, Iowa, 52242, USA.*

10 PRESENT ADDRESS: ²Biosciences Division, Argonne National Laboratory, Argonne, Illinois,
11 60439, USA.

Submitted to: *Environmental Science and Technology*

13 *Corresponding Author

14 Biosciences Division

15 Argonne National Laboratory

16 9700 S. Cass Avenue

17 Argonne, IL 60439

18 Phone: (630)252-3985

19 E-mail: dlatta@anl.gov

20 **Methods and Materials**

21 **Goethite Synthesis.** Goethite was synthesized from naturally abundant iron with and without
22 aluminum substitution by modifying previously described methods and summarized in Table
23 S1.¹⁻² All solutions and suspensions were prepared in HDPE plastic bottles to avoid silicate
24 contamination from glassware. To start, a solution of Al(NO₃)₃·9H₂O was added to 5 M KOH to
25 create 0.313 M soluble aluminate Al(OH)₄⁻ in 1.88 M KOH. Aluminate solution was added to 1
26 L bottles containing enough 5 M KOH to make a total of 1 L of 0.3 M KOH at no and low Al
27 concentrations [Al/(Al+Fe) < 0.27] or 1.0 M KOH at higher Al concentrations. Ferric iron was
28 added to the aluminate solution as 50 mL of 1 M Fe(NO₃)₃·9H₂O, and the Fe(III)-Al precipitate
29 suspension was diluted to 1 L. Al-free suspensions were aged for 72 hours at 70 °C and Al-
30 containing suspensions were aged at 60 °C for 4 weeks. After aging, the solids were centrifuged
31 and the supernatant was discarded. The solids were washed once with 1 M KOH to remove any
32 Al precipitates and centrifuged. The goethite was resuspended in DI water and adjusted to a pH
33 of approximately 9.0 with 1 M HCl to increase flocculation, and washed three times by
34 centrifugation. Uncrystallized material was then removed by dissolution in 0.5 M HCl for 2
35 hours, and the solids were washed 3 times, dried, and powdered.

36 Goethite with and without aluminum substitution was also synthesized from ⁵⁶Fe
37 (Mössbauer silent) in order to investigate electron transfer dynamics between ⁵⁷Fe(II)
38 (Mössbauer active) and the underlying goethite. The synthesis parameters and properties are
39 outlined in Table S1 and are similar to the above procedures. Goethite was synthesized by
40 dissolving ⁵⁶Fe(0) powder (Chemgas, Inc., 99.77%) in 25 mL of 1 M HCl. The resulting 200 mM
41 ⁵⁶Fe(II) containing solution was oxidized to ⁵⁶Fe(III) with excess H₂O₂. For ⁵⁶Fe Al-goethite, an
42 AlCl₃ aluminate solution and 25 mM ⁵⁶Fe(III) were used. Total volume was 100 mL, and all

43 other parameters were used as described above and in **Table S1**. The suspensions were aged at
44 60 °C in an oven for 3 months in order to insure complete conversion of the Fe(III)/Al precipitate
45 to goethite. The ⁵⁶Fe Al-goethite was synthesized in parallel with naturally-abundant Fe(0)
46 powder for Mössbauer analysis. After aging, the goethite was processed by washing once with 1
47 M KOH, then 3 times with DI water, dried, and ground to a powder. A similar procedure was
48 followed for Al-free ⁵⁶Fe goethite, with aluminate solution omitted and 0.3 M KOH.

49 **Goethite Characterization.** Al and Fe content of the goethites were measured by dissolution in
50 8 M HCl overnight at 70 °C, and measuring Al and Fe using ICP-OES or ICP-MS. Al content as
51 Al/(Al+Fe) of the naturally abundant Fe goethite used in this study was 9.9% (10% Al-goethite).
52 The Al contents of the ⁵⁶Fe Al-goethites used in this study were 5.4% and 9.4%, these are
53 referred to as “⁵⁶Fe Al-goethite (5%)” and “⁵⁶Fe Al-goethite (9%)”, respectively. In addition, a
54 proton promoted kinetic dissolution experiment was done on the 10% Al-goethite at room
55 temperature (22 °C) and the congruency of Al and Fe dissolution were measured using ICP-MS
56 (**Figure S4**). Insufficient material was present from the ⁵⁶Fe goethites to measure dissolution
57 time courses, but an Al-goethite with 4.4% substitution prepared from natural Fe dissolved
58 congruently (data not shown).

59 All of the goethites used in the study have been characterized with powder x-ray
60 diffraction (pXRD) to determine if phases other than goethite were present (**Figure S2**). All data
61 was collected using a Rigaku Mini FlexII diffractometer using Co K-alpha radiation with a K-
62 beta filter made from Fe. No secondary phases were noted in any of the goethites used. In order
63 to discuss the goethite crystal structure, we have chosen to use the Pbnm space group indexing,
64 as it can be used to directly compare our results to the majority of the work investigating Al-
65 substitution in goethite. Some more recent work uses the Pnma space group.³ The Pbnm space

group (*abc*) can be translated to the Pnma space group with the following transformation: (*abc*) → (*bca*). Using the pXRD patterns we measured the full width at half maximum (FWHM) of (111) and (110) planes of the goethite crystal lattice using the Jade 6 software package (Materials Data, Incorporated, USA). The FWHM of these planes was used in the Scherrer equation to calculate the mean crystallite dimension (MCD).⁴, and references therein The *c*-dimension of the Al-goethite unit cells was calculated using the whole-pattern fitting procedure in the Jade 6 software package, and used to estimate the aluminum content of these goethites.⁴

The goethites used in this study were also imaged with scanning electron microscopy (SEM) (Hitachi S-4800). This was used to provide images of the particle size and morphology of the goethite particles, and to check for secondary phases that may have been missed by low concentration in pXRD (**Figure S3**). Particles were suspended in deionized water (DI), sonicated briefly with a probe sonicator, and dropped onto aluminum sample stubs. Accelerating voltages of 1.0 – 5.0 kV gave high quality images without the need to sputter coat with Au or carbon.

Mössbauer Spectroscopy. Transmission Mössbauer spectroscopy was done with a variable temperature He-cooled system with a 1024 channel detector. A ⁵⁷Co source (~ 50 mCi) embedded in Rh was used and was maintained at room temperature. All center shifts reported are calibrated relative to an α-Fe foil at room temperature. Samples are kept anoxic by mounting them between pieces of adhesive Kapton tape, and minimizing the time they are exposed to air prior to mounting them in the spectrometer cryostat. Collected Mössbauer spectra have been fit using the Recoil software package (University of Ottawa, Ottawa, Canada) using Voigt based fitting. The relative peak areas of the sextets have been set with the ideal proportions of 3:2:1:1:2:3. Center shift (CS), quadrupole shift (QS), and hyperfine field (H) parameters have been allowed to float during the fitting procedure unless otherwise noted. Mössbauer

89 spectroscopy was used characterize the goethites used and check for Fe containing impurities in
90 samples containing ^{57}Fe . Also, ^{56}Fe goethite and Al-goethite samples were checked for the
91 presence of significant ^{57}Fe at 15K, and found to be lacking of measurable quantities of the
92 Mössbauer active isotope.

Table S1. Properties of pure and Al-substituted goethites used in this study (\pm 1 standard deviation, when given).

Sample ID	Synthesis Parameters					Solid properties					
	Initial Al/(Al+Fe)	[KOH] (M)	Temp. (°C)	Aging Time (week)	Al/(Al+Fe) ^a solid x 100%	MCD ₍₁₁₀₎ ^b (nm)	MCD ₍₁₁₁₎ ^c (nm)	Length (nm) (n = 15)	Width (nm) (n = 15)	pXRD Al Content ^d	BET Surface area (m ² /g)
Large Batch Natural Fe Goethites											
Micro-goethite	0	0.3	70	0.4	0	26	34	1090 \pm 740 (n = 38)	166 \pm 91 (n = 53)	n.m.	20
Nano-goethite	0	pH 12	90	0.14	0	n.m.	n.m.	95 \pm 37	14 \pm 5	n.m.	117
10Al-goethite	0.44	1.0	60	4	9.85 \pm 0.03 ^e	49	90	416 \pm 153	158 \pm 99	12	7.9
Small Batch ⁵⁶ Fe Al-Goethites											
⁵⁶ Fe Goethite (Batch 1) ^f	0	0.3	70	2	0	16	28	n.m. ⁱ	n.m. ⁱ	2.1	n.m. ⁱ
⁵⁶ Fe Goethite (Batch 2) ^g	0	0.3	70	2	0	34	50	n.m.	n.m.	1.2	n.m.
⁵⁶ Fe Al-Goethite (5%)	0.27	1.0	60	14	5.41 ^h	19	28	993 \pm 370	109 \pm 28	7.5	n.m.
⁵⁶ Fe Al-Goethite (9%)	0.44	1.0	60	14	9.44 ^h	30	49	569 \pm 180	103 \pm 29	12	n.m.

^a = Percent (%) aluminum substitution determined by dissolution in HCl and measurement with ICP-OES.

Table S1—continued

^{b, c} = Mean crystallite dimensions (MCD) determined from pXRD data of the breadth of the (110) and (111) reflections of goethite.

^d = Powder XRD determined Al content using the equation described in Ref.⁴. The method has a 95% CI of $\pm 2.6\%$ Al.

^e = Mean and 1 standard deviation of triplicate reactors of 10 mg of goethite dissolved in 8 M HCl.

^f = Used for 1 mM $^{57}\text{Fe}(\text{II})$ experiment, all phosphate experiments, and phospholipid experiment.

^g = Used for 3 mM $^{57}\text{Fe}(\text{II})$ experiment, and all other anion experiments (NOM, SiO_4^{4-} , CO_3^{2-}).

^h = Average of duplicates of 10 mg goethite dissolved in 8 M HCl.

ⁱ = not measured.

Table S2: Experimental conditions for Fe(II) to goethite electron transfer experiments in the presence of sorbed anions.

Experiment ID	Solution Conditions	[Anion] initial (mM)	Anion Uptake after Sorption (mM) ^a	Total Anion Uptake (mM) ^b	[Fe(II)] initial (mM)	Fe(II) uptake (mM)	pH, initial ^c	pH, final	Mössbauer spectroscopy figure
P/Low Fe(II)	10 mM KCl	0.51	0.175	0.192	0.125	0.113	7.51	7.64	Figure 1D
P/High Fe(II)	10 mM KCl	0.491	n.m. ^d	0.206	0.25	0.233	7.55	7.54	Figure 1E
Bicarbonate	10 mM KCl	4.0	n.m. ^d	n.m. ^d	1.16	0.266	7.54	7.28	Figure 1F
Low Silicate	10 mM KCl	1.0	n.m. ^d	n.m. ^d	1.14	0.191	7.46	7.17	Figure 1G
High Silicate	10 mM KCl	10.0	n.m. ^d	n.m. ^d	1.38	0.303	7.52	6.84	Figure 1H
Natural Organic Matter (NOM)	10 mM KCl	20 mg L ⁻¹	n.m. ^d	n.m. ^d	1.14	0.263	7.48	7.02	Figure 1I
Phospholipid (DOPA)	25 mM HEPES/25 mM KBr	1.0	n.m. ^d	n.m. ^d	~1	~0.7	7.51	7.51	Figure 1J

^a Anion uptake from solution by 2 g L⁻¹ goethite after equilibration but prior to addition of ⁵⁷Fe(II).

^b Total anion uptake from solution by 2 g L⁻¹ goethite after addition of ⁵⁷Fe and a period of equilibration.

^c pH after re-adjustment following the spike of ⁵⁷Fe(II) to solution.

^d not measured

Table S3. Mössbauer parameters derived from fitting spectra recorded at 77 K for ^{56}Fe goethite, ^{56}Fe Al-goethite, and ^{56}Fe goethite with sorbed anions reacted with $^{57}\text{Fe}(\text{II})$. Al-goethite samples reacted for 20 hours, and samples with anions reacted for 4-8 hours.

Component	CS ^a (mm s ⁻¹)	QS ^b (mm s ⁻¹)	H ^c (Tesla)	std(H) ^d (T) or std(QS) ^e (mm s ⁻¹)	Area (%)
Goethite					
Sextet	0.48	-0.24	49.5	0.77	100
^{56}Fe Goethite + 1 mM $^{57}\text{Fe}(\text{II})$					
Sextet 1	0.47	-0.34 ^f	48.9	0.84	45
Sextet 2	0.52	0.16	49.2	0.99	27
Collapsed Feature	0.50	-0.35	27.8	14*	27
Fe(II) Doublet	1.15	2.76	-	0.24	1
^{56}Fe Al-Goethite (5%) + 1 mM $^{57}\text{Fe}(\text{II})$					
Sextet 1	0.47	-0.36 ^f	48.5	1.0	41
Sextet 2	0.52	0.13	48.7	1.2	26
Collapsed Feature	0.46	-0.04	28.9	12*	28
Fe(II) Doublet	1.28	2.4	-	0.63	5
^{56}Fe Al-Goethite (9%) + 1 mM $^{57}\text{Fe}(\text{II})$					
Sextet 1	0.48	-0.38 ^f	48.1	1.5	35
Sextet 2	0.49	0.09	48.1	1.6	26
Collapsed Feature	0.39	-0.26	32.0	12	31
Fe(II) Doublet	1.25	2.41	-	0.63	8
^{56}Fe Goethite + 3 mM $^{57}\text{Fe}(\text{II})$					
Sextet 1	0.47	-0.25	48.9	0.79	43
Sextet 2	0.53	0.14	49.5	1.06	24
Collapsed Feature	0.44	-0.14	29.3	14.4*	28
Fe(II) Doublet	1.26	2.66	-	0.36	4
Fe(III) Doublet	0.65	0.27	-	0.16	1
^{56}Fe Al-Goethite (5%) + 3 mM $^{57}\text{Fe}(\text{II})$					
Sextet 1	0.47	-0.46 ^t	48.4	1.23	30
Sextet 2	0.50	0.06	48.7	1.38	31
Collapsed Feature	0.37	-0.18	30.8	14.5*	34
Fe(II) Doublet	1.25	2.53	-	0.48	5
^{56}Fe Al-Goethite (9%) + 3 mM $^{57}\text{Fe}(\text{II})$					
Sextet 1	0.47	-0.48 ^t	48.0	1.35	30
Sextet 2	0.50	0.06	48.1	1.46	30
Collapsed Feature	0.38*	-0.18*	30.7	14.5*	33
Fe(II) Doublet	1.26	2.64	-	0.57	7
^{56}Fe Goethite + 0.51 mM Phosphate + 0.13 mM $^{57}\text{Fe}(\text{II})$					
Sextet 1	0.47	-0.42 ^f	48.8	0.98	33
Sextet 2	0.50	0.10	49.1	0.93	30
Collapsed Feature	0.43	-0.42	30.5	14.5*	32
Fe(II) Doublet	1.36	2.92	-	0.53	6
^{56}Fe Goethite + 0.5 mM Phosphate + 0.28 mM $^{57}\text{Fe}(\text{II})$					
Fe(II) Doublet 1	1.29	2.65	-	0.31	32
Fe(II) Doublet 2	1.36	3.23	-	0.18	28
Sextet 1	0.47	-0.22	48.4	1.75	18
Sextet 2	0.48	0	49.4	1.40	22
^{56}Fe Goethite + ~1 mM DOPA phospholipid + 1 mM $^{57}\text{Fe}(\text{II})$					
Fe(II) Doublet	1.38	2.90	-	-	100
Vivianite ^g					
Fe(II) Doublet 1	1.33	3.14	-	-	- ^g
Fe(II) Doublet 2	1.27	2.54	-	-	- ^g

Table S3—Continued.

* Denotes that the parameter was fixed during the fitting procedure to obtain resonable values for the Mössbauer hyperfine parameters.

^a Center shift.

^b Quadrupole splitting for doublets and quadrupole shift parameter for sextets.

^c Hyperfine field.

^{d,e} Standard deviation of the Voigt profile for the hyperfine field or quadrupole splitting parameters, respectively.

^f Note the deviation in the quadrupole shift parameter for Sextet 1 relative to goethite.

^g Ref ⁵, relative areas not reported.

Table S4. ^{54}Fe isotope data during for Fe isotope tracer experiments between aqueous Fe(II) and goethite, Al-goethite, and goethite with sorbed phosphate.

Aqueous ^{54}Fe		
Time (d)	$f^{54}\text{Fe}$	% exchange ^a
Goethite (2 g/L) + 1 mM Fe(II)		
0	0.002 (0.0001) ^b	0 (0) ^b
0.007	0.012 (0.0009)	23.7 (2.0)
0.083	0.017 (0.0003)	32.7 (0.61)
0.625	0.022 (0.0008)	44.3 (1.9)
1.6	0.022 (0.0021)	45.7 (4.6)
3.0	0.027 (0.0039)	55.3 (8.6)
6.0	0.024 (0.0001)	49.7 (0.14)
14.2	0.023 (0.0019)	46.4 (4.1)
31.25	0.020 (0.0006)	41.2 (1.1)
Al-goethite (2 g/L) + 1 mM Fe(II)		
0	0.001 (0.0002)	0 (0)
0.021	0.001 (0.0001)	0.76 (0.30)
0.083	0.004 (0.0019)	5.58 (3.7)
0.667	0.003 (0.0006)	5.42 (1.2)
1.5	0.003 (0.0001)	4.66 (0.50)
3.0	0.003 (0.0001)	5.81 (0.62)
6.1	0.004 (0.0009)	6.71 (1.5)
14.7	0.007 (0.0039)	11.8 (8.4)
31.1	0.005 (0.0010)	8.54 (2.3)
Nano-goethite (1 g/L) + 0.1 mM Fe(II)		
0	0.006 (0.002)	0 (0)
0.007	0.020 (0.0004)	33.7 (0.8)
3	0.032 (0.0009)	55.1 (1.6)
10	0.044 (0.0007)	75.6 (1.2)
16	0.045 (0.0004)	76.9 (0.6)
21	0.045 (0.0001)	77.4 (0.1)
Nano-goethite (1 g/L) + 0.35 mM PO ₄ + 0.1 mM Fe(II)		
0	0.0057 (0.002)	0 (0)
0.007	0.016 (0.005)	18.8 (4.4)
0.5	0.039 (0.016)	64.2 (14.8)
1	0.041 (0.008)	66.6 (8.9)
3	0.051 (0.002)	86.0 (2.4)
10	0.052 (0.0001)	89.1 (0.2)
16	0.053 (0.0001)	90.7 (1.8)
21	0.053 (0.0003)	91.2 (0.5)

^a % exchange calculated using eq 2 in the text.

^b Standard deviation measured from triplicate reactors.

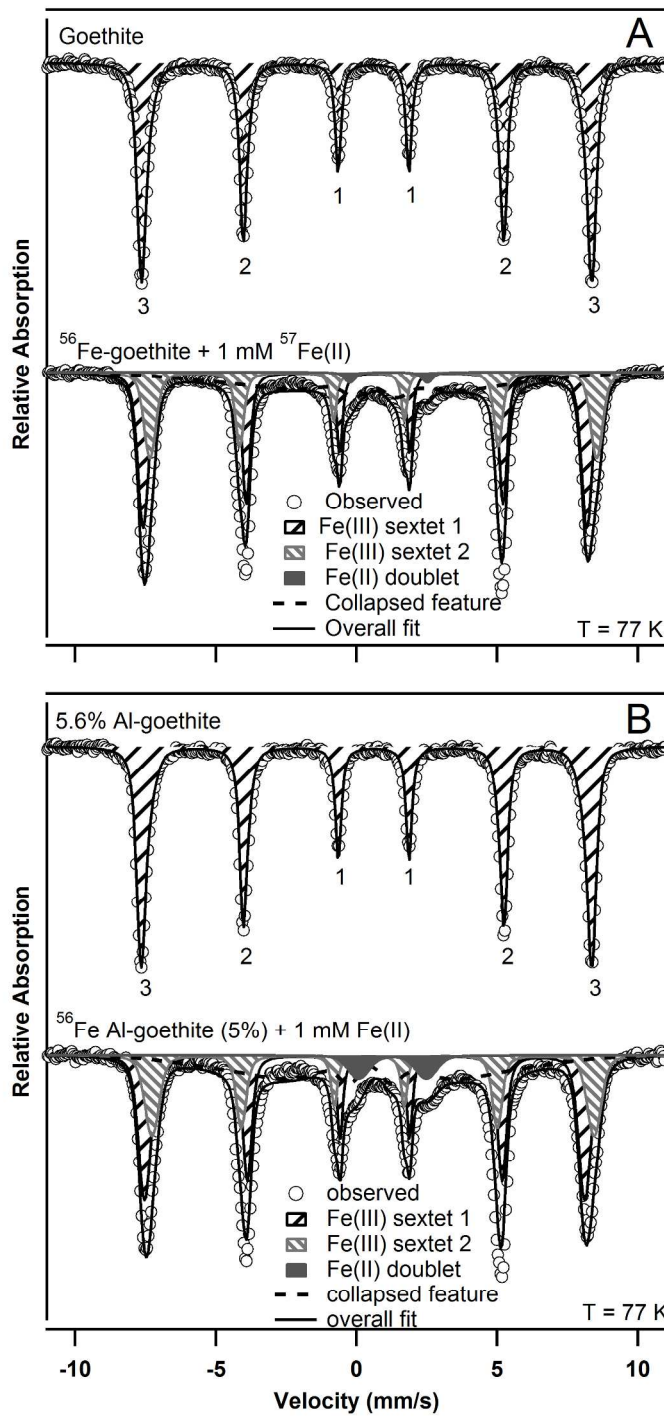


Figure S1. Mössbauer spectral fits of (A) naturally abundant goethite (top spectrum) and ^{56}Fe goethite reacted with 1 mM $^{57}\text{Fe}(\text{II})$ (bottom spectrum). (B) naturally abundant Al-goethite (5.6% Al) (top spectrum) ^{56}Fe Al-goethite (5% Al) reacted with 1 mM $^{57}\text{Fe}(\text{II})$. The peaks of the corresponding unreacted goethite sextets are labeled with the ideal 3:2:1:1:2:3 area ratios. Spectral parameters are reported in **Table S3**.

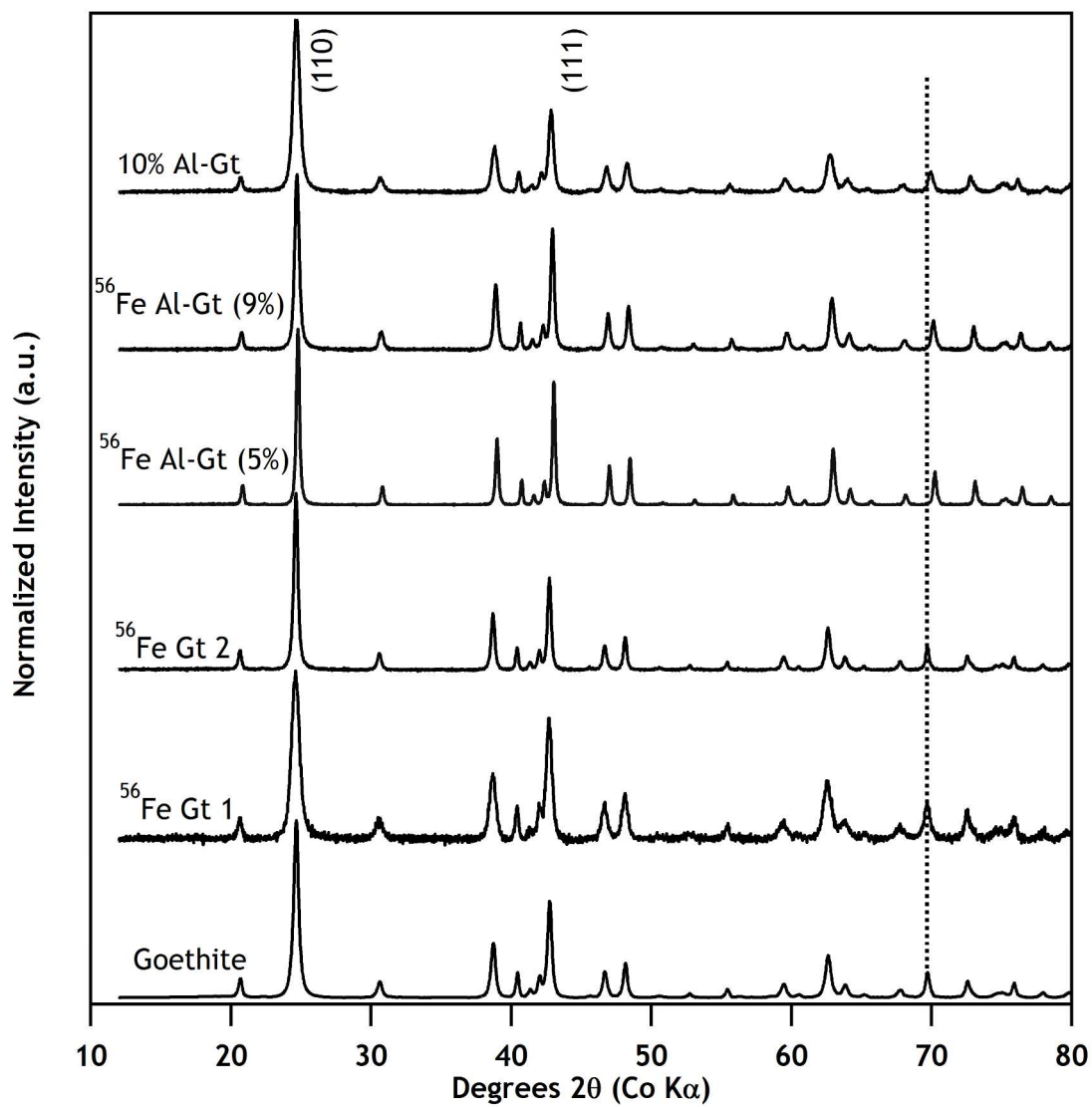


Figure S2. Powder x-ray diffraction patterns of the goethite (Gt) and Al-goethite (Al-Gt) used in this study. The dotted vertical line is shown as a visual reference to the change in goethite crystal properties upon aluminum substitution.

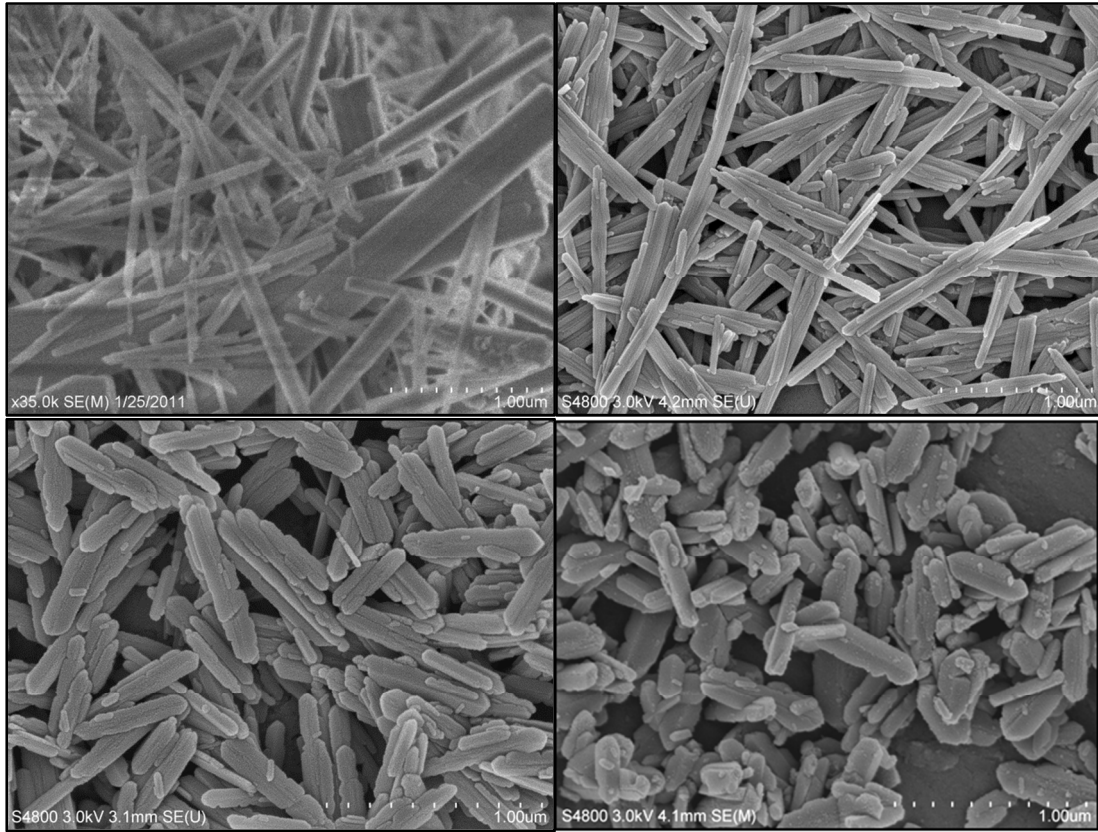


Figure S3. Scanning electron micrographs (SEMs) of (clockwise from top left) goethite, ^{56}Fe Al-goethite (5%), ^{56}Fe Al-goethite (9%), and 10% Al-goethite showing the change in morphology of the goethite particles with increasing aluminum content.

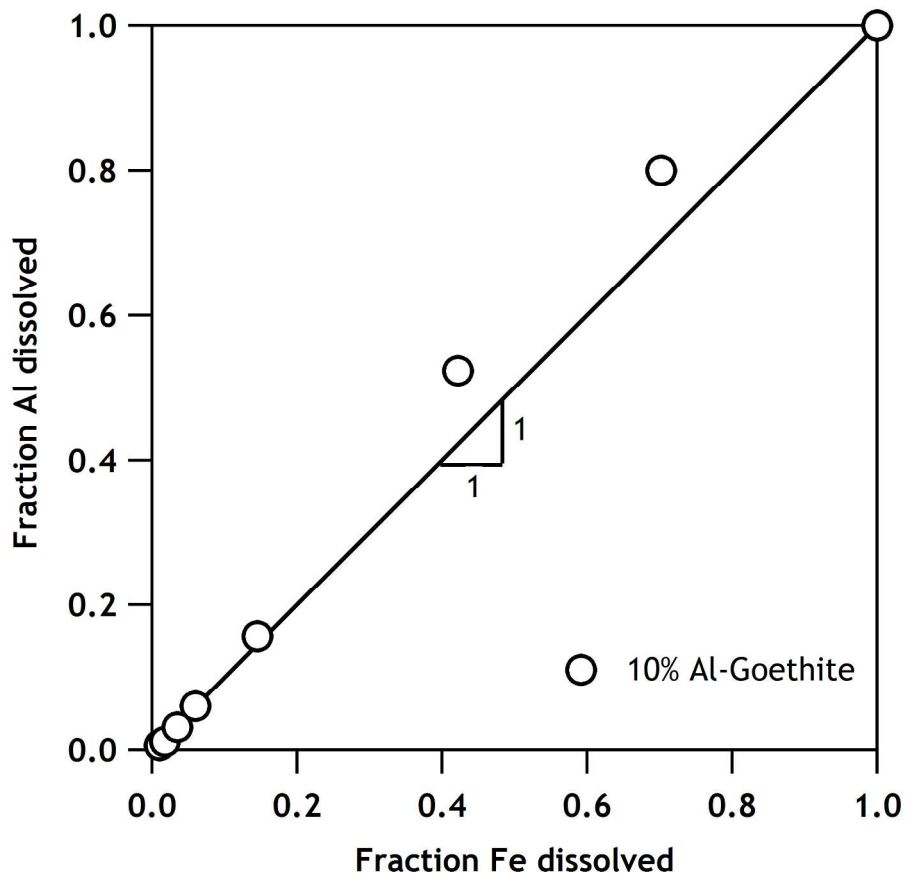


Figure S4. Dissolution of naturally abundant Fe 10% Al-goethite in 8 M HCl. Congruent dissolution is represented by the solid line.

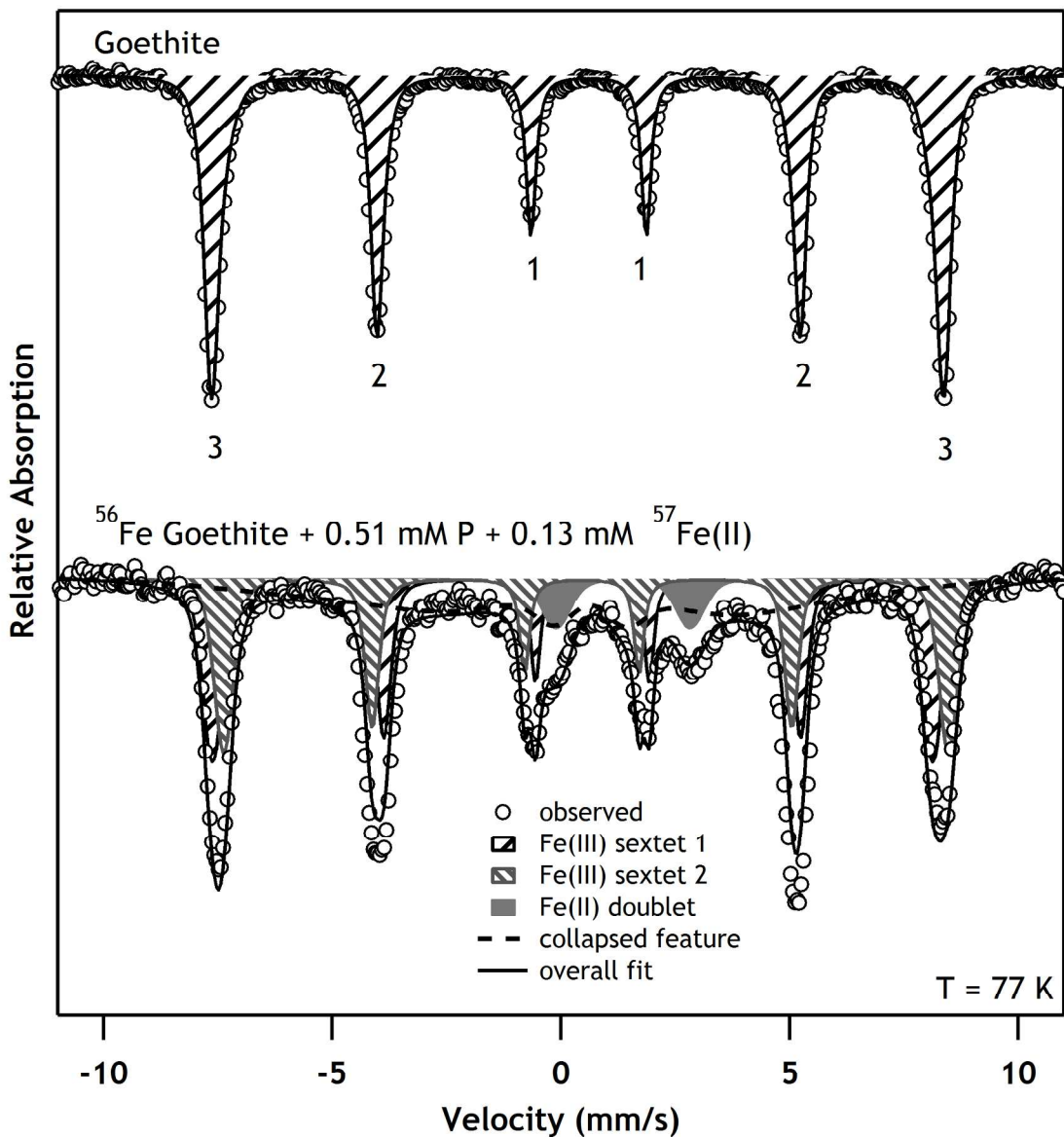


Figure S5: Fitted Mössbauer spectrum of 0.13 mM $^{57}\text{Fe}(\text{II})$ reacted with 2 g L^{-1} ^{56}Fe goethite with 0.5 mM pre-sorbed phosphate. The spectrum was fit with two Fe(III) sextets (black and grey hatched components), an Fe(II) doublet (solid grey), and a poorly resolved collapsed feature (dashed line). Unreacted goethite was fit with only one sextet. Parameters from fitting are reported in **Table S3**.

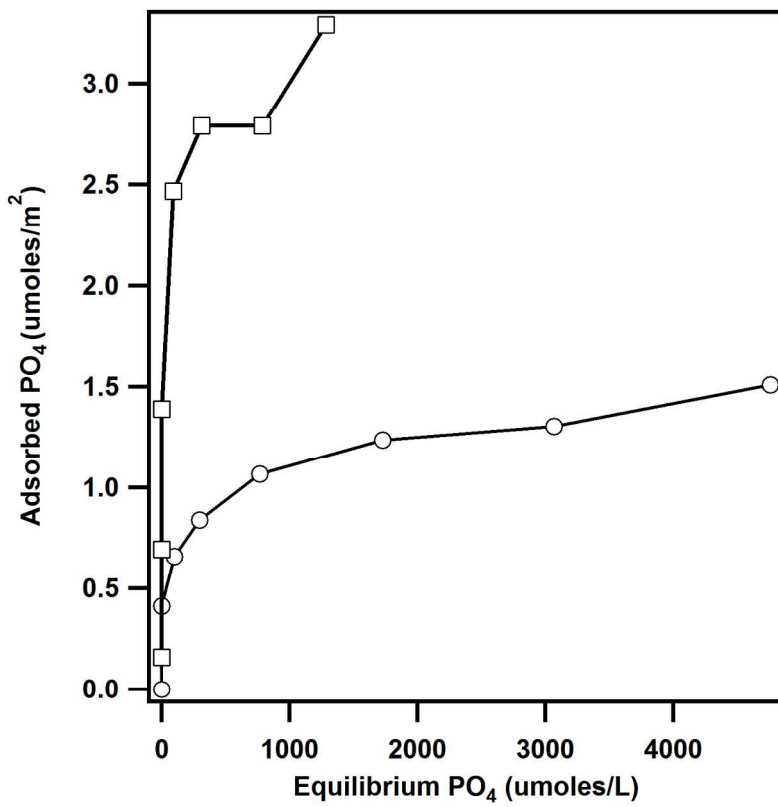


Figure S6. Phosphate sorption onto 1 g/L nano-goethite at a pH value of 7.5 in 10 mM KCl background electrolyte (open circles) and 2 g/L of micro-goethite under the same conditions (open squares) with no added Fe(II).

References

- (1) Lewis, D. G.; Schwertmann, U., Influence of Aluminum on the Formation of Iron-Oxides .4. Influence of [Al], [OH], and Temperature. *Clays Clay Miner.* **1979**, 27 (3), 195-200.
- (2) Schwertmann, U.; Cornell, R. M., *Iron Oxides in the Laboratory: Preparation and Characterization*. 2nd ed.; Wiley-VCH: New York, 2000; p 188.
- (3) Cornell, R. M.; Schwertmann, U., *The Iron Oxides: Structure, Properties, Reactions, Occurrences and Uses* 2nd ed.; Wiley-VCH: Weinheim, Germany, 2003; p 664.
- (4) Schulze, D. G., The Influence of Aluminum on Iron-Oxides .8. Unit-Cell Dimensions of Al-Substituted Goethites and Estimation of Al from Them. *Clays Clay Miner.* **1984**, 32 (1), 36-44.
- (5) Forsyth, J. B.; et al., The magnetic structure of vivianite, $\text{Fe}_3(\text{PO}_4)_2 \cdot 8\text{H}_2\text{O}$. *J. Phys. C* **1970**, 3 (5), 1127.